

Western  Graduate&PostdoctoralStudies

Western University
Scholarship@Western

Electronic Thesis and Dissertation Repository

1-18-2013 12:00 AM

Subcellular Analysis of the Disulfide Proteome in p66Shc expressing Nerve Cells

Tyler Cann
The University of Western Ontario

Supervisor
Dr. Robert Cumming
The University of Western Ontario

Graduate Program in Biology
A thesis submitted in partial fulfillment of the requirements for the degree in Master of Science
© Tyler Cann 2013

Follow this and additional works at: <https://ir.lib.uwo.ca/etd>

 Part of the [Biology Commons](#), and the [Cell Biology Commons](#)

Recommended Citation

Cann, Tyler, "Subcellular Analysis of the Disulfide Proteome in p66Shc expressing Nerve Cells" (2013).
Electronic Thesis and Dissertation Repository. 1123.
<https://ir.lib.uwo.ca/etd/1123>

This Dissertation/Thesis is brought to you for free and open access by Scholarship@Western. It has been accepted for inclusion in Electronic Thesis and Dissertation Repository by an authorized administrator of Scholarship@Western. For more information, please contact wlsadmin@uwo.ca.

Subcellular Analysis of the Disulfide Proteome in p66Shc expressing Nerve Cells

By

Tyler D. Cann

Graduate Program in Biology

A thesis submitted in partial fulfillment
of the requirements for the degree of

Master of Science

The School of Graduate and Postdoctoral Studies

The University of Western Ontario

London, Ontario, Canada

© Tyler D. Cann 2013

CERTIFICATE OF EXAMINATION

Supervisor

Examiners

Dr. Robert Cumming

Dr. Sashko Damjanovski

Supervisory Committee

Dr. Greg Kelly

Dr. Dean Betts

Dr. Denis Maxwell

Dr. Greg Kelly

Dr. Robert Dean

The thesis by

Tyler Douglas Cann

entitled:

**Subcellular Analysis of the Disulfide Proteome in p66Shc
expressing Nerve Cells**

is accepted in partial fulfillment of the
requirements for the degree of
Master of Science

Date

Chair of the Thesis Examination Board

Abstract

The longevity associated protein p66Shc has been suggested to regulate organismal lifespan through initiation of apoptotic pathways. Following stress-induced translocation into the mitochondria, p66Shc promotes increased reactive oxygen species (ROS) production and triggers poorly defined downstream signaling events that lead to decreased cell viability. Protein disulfide bonding has recently emerged as a ROS dependent post-translational modification that regulates protein function and signaling processes. Using the mouse hippocampal HT-22 cell line, I sought to determine the changes in the disulfide proteome associated with p66Shc mediated ROS production. Through Redox 2D-SDS PAGE analysis of mitochondrial and cytosolic extracts, redox sensitive proteins altered by p66Shc mediated ROS formation were identified. Of specific interest to this study, lamin B1 (LMNB1) and peroxiredoxin1 (PRXI) were identified as proteins that underwent an alteration in redox status and localization to the mitochondria in a p66Shc dependent manner. Furthermore, cytoskeletal proteins moesin, radixin tropomyosin-3 (TPM-3) and adenylate cyclase associated protein 1 (CAP1) were identified as undergoing changes in disulfide bonding in response to p66Shc mediated ROS production. The disulfide altered proteins identified in this study are generally associated with maintaining ROS balance and regulating cytoskeletal actin dynamics. Recent studies suggest these proteins may also acquire secondary roles involved in stress response and apoptotic pathways. My findings reveal that p66Shc elicits redox signaling events via ROS-dependent disulfide bonding of key antioxidant and cytoskeletal regulatory proteins which may affect apoptotic processes associated with organismal and cellular aging.

Key Words: p66Shc, ROS, redox, apoptosis, disulfide bond.

Acknowledgements

Firstly, I would like to express many thanks to my supervisor, Dr. Robert Cumming for his mentorship and motivation in my late undergraduate years and throughout my graduate studies. Without his support and confidence in me over the past few years, this research and my appreciation for science would not exist, for that I am forever grateful.

I would like to thank Dr. Dean Betts and Dr. Greg Kelly for their assistance and advice throughout my project. Their questions and comments provided direction and helped me overcome many obstacles during my research.

I would like to extend many thanks to the Cumming Lab students, past and present, for their patience, support and enthusiasm regarding their own research endeavours and mine. This research would not be possible without them.

A very special thanks to Robert (Bobby) Arsenault and Mark Fox for their unrivaled support and friendship throughout my graduate studies and for the positive impact they have had on my life generally. Thanks to Jordan Newington for all her support, and for helping me see the lighter side of almost any situation.

I owe so much gratitude to my parents, Doug and Kathryn. Their love, support, countless sacrifices and belief in me has allowed me to achieve my goals in all facets of life. To my brother Trevor, for being so supportive and giving me inspiration to succeed through his own achievements. Finally, special thanks to my grandparents, for helping me appreciate the value of higher education and supporting me throughout all of my endeavours.

Table of Contents

CERTIFICATE OF EXAMINATION.....	ii
ABSTRACT.....	iii
ACKNOWLEDGEMENTS.....	iv
TABLE OF CONTENTS.....	v
LIST OF TABLES.....	vi
LIST OF FIGURES.....	vii
LIST OF ABBREVIATIONS.....	viii
1. INTRODUCTION.....	1
1.1 Overview.....	1
1.2 Reactive Oxygen Species.....	1
1.3 Shc Protein Family and the p66Shc Isoform.....	3
1.4 Regulatory Mechanisms of Protein Disulfide Bonds.....	6
1.5 Cell Stress Responses and Rationale.....	8
1.6 Hypothesis and Research Outline.....	9
2. MATERIALS AND METHODS.....	13
2.1 Cell Culture Conditions	13
2.2 HA-tagged p66Shc Vector Construction	13
2.3 Transfection and Activation of HA-tagged p66Shc	14
2.4 Conventional SDS PAGE and Immunoblot Analysis	15
2.5 Mitochondrial ROS Analysis	16
2.6 Trypan Blue Exclusion Test	17
2.7 HT-22 Subcellular Fractionation and Mitochondrial Isolation	17
2.8 Redox 2D SDS PAGE Analysis	18
2.9 Silver Staining of Redox 2D Gels	19
2.10 Identification of Redox Sensitive Proteins.....	19
2.11 TRITC-Phalloidin Immunostaining of Actin Filaments.....	20
2.12 Non-Reducing/Reducing 1D SDS PAGE	21
2.13 Statistical Analysis.....	22
3. RESULTS.....	23
3.1 Production and Expression of HA-tagged p66Shc Expression Construct	23
3.2 Phosphorylation of p66Shc using the PKC- β Agonist DOPPA	23
3.3 p66Shc Activation Increases Mitochondrial ROS Production	24
3.4 p66Shc Activation Decreases Cell Viability	29
3.5 p66Shc Mediated Changes in the Mitochondrial Disulfide Proteome	34
3.6 Identifying Mitochondrial-associated DSBPs Altered with p66Shc Activation ..	34
3.7 Identification of Cytosolic DSBPs Altered with p66Shc Activation	35
3.8 p66Shc Activation affects Redox Status of Tropomyosin-3 in the Cytosol	42
3.9 Changes in Filamentous Actin Organization following p66Shc Activation	42

4. DISCUSSION AND FUTURE RESEARCH.....	48
4.1 Overview.....	48
4.2 p66Shc Phosphorylation Increases ROS and Decreases Cell Viability.....	48
4.3 p66Shc Mediated Alterations in the Mitochondrial Disulfide Proteome.....	49
4.3.1 Lamin B1.....	50
4.3.2 Peroxiredoxin I.....	51
4.3.3 Eukaryotic Elongation Factor 1 Alpha 1.....	52
4.4 p66Shc Mediated Alterations on the Cytosolic Disulfide Proteome	52
4.4.1 Moesin and Radixin.....	52
4.4.2 Cyclase Associated Protein.....	53
4.4.3 Tropomyosin-3.....	53
4.5 Non-reducing/Reducing Behaviour of Tpm-3 in p66Shc Expression Samples...54	
4.6 Cytoskeleton Structure Changes with Cytosolic DSBP Alterations.....	55
4.7 Conclusions.....	57
REFERENCES.....	59
CURRICULUM VITAE.....	64

List of Abbreviations

ATP	Adenosine Triphosphate
BME	Beta mercaptoethanol
CH1	Collagen Homology domain 1
CH2	Collagen Homology domain 2
Cys-S ⁻	Thiolate Anion
DMSO	Dimethyl Sulfoxide
DSB	Disulfide Bond
DSBP	Disulfide Bonded Protein
EGF	Epidermal Growth Factor
ETC	Electron Transport Chain
FBS	Fetal Bovine Serum
H ₂ O ₂	Hydrogen Peroxide
HPETE	Hydroperoxyeicosatetraenoic acid
HMW	Higher Molecular Forms
IA	Iodoacetamide
IGF-1	Insulin-like Growth Factor 1
IMS	Intermembrane Space
kDa	Kilo Dalton
MPT	Mitochondrial Permeability Transition
mM	MilliMolar
MS	Mass Spectrometry
NADP ⁺	Nicotinamide Adenine Dinucleotide Phosphate

NADH	Nicotinamide Adenine Dinucleotide (Reduced)
NaF	Sodium Fluoride
Na ₃ VO ₄	Sodium Orthovanadate
nM	Nano Molar
NOX	NADPH Oxidase
O ₂	Molecular Oxygen
O ₂ ⁻	Superoxide Anion
PAGE	Polyacrylamide Gel Electrophoresis
PCR	Polymerase Chain Reaction
PKC-β	Protein Kinase C-β
PMSF	Phenylmethanesulfonylfluoride
PVDF	Polyvinylidene Fluoride
PRX	Peroxiredoxin
PTB	Phosphotyrosine Binding Domain
ROS	Reactive Oxygen Species
SH2	Src Homologous type 2 domain
Shc	Src Homologous and Collagen-like
SOD1	Superoxide Dismutase 1
SOD2	Superoxide Dismutase 2
SRX	Sulfiredoxin
UV	Ultraviolet
VDAC	Voltage Dependent Anion Channel
ΔΨ _m	Mitochondrial Membrane Potential

List of Figures

Figure 1	Model of p66Shc mediated mitochondrial ROS production.....	11
Figure 2	Analysis of endogenous and ectopically expressed p66Shc levels in HT-22 cells.....	25
Figure 3	Optimization of p66Shc phosphorylation in HT-22 cells transfected with p66Shc-expressing plasmids.....	27
Figure 4	Effect of p66Shc phosphorylation on mitochondrial ROS production in HT-22 cells.....	30
Figure 5	The effect of p66Shc-HA activation on cell viability in HT-22 cells	32
Figure 6	Ectopic p66Shc overexpression alters the mitochondrial disulfide proteome in HT-22 cells.....	36
Figure 7	Ectopic p66Shc overexpression alters the disulfide proteome in HT-22 cytosolic fractions.....	39
Figure 8	Overexpression of p66Shc-HA promotes increased disulfide linkage of cytosolic Tpm-3.....	44
Figure 9	p66Shc activation in HT-22 cells promotes alterations in F-actin consistent with altered disulfide bonding of cytosolic regulators.....	46

List of Tables

Table 1	Identification of mitochondrial disulfide linked Proteins altered by p66Shc overexpression and DOPPA (50 Nm) treatment.....	38
Table 2	Identification of cytosolic disulfide linked proteins Altered by p66Shc overexpression and DOPPA (50 nM) Treatment.....	46

Chapter 1

Introduction

1.1 Overview

Aging is regarded as a natural biological process that occurs in all living organisms, however the cellular and molecular mechanisms underlying aging are not well understood. Cellular aging is associated with changes in gene expression, mutations, and elevated risk of apoptosis (Lombard et al., 2005). There is also evidence that the efficiency of cellular processes decrease over time, such that metabolism, protein function and oxygen by-products are altered as cells age (Sohal & Orr, 2012). The free radical theory of aging posits that there is increased formation of intracellular oxygen radicals primarily derived from mitochondria. This theory suggests that imperfections in the mitochondrial electron transport chain (ETC) during oxidative metabolism results in the formation and accumulation of partially reduced oxygen over time (Beckman & Ames, 1998). Partially reduced molecular oxygen can subsequently be converted to membrane permeable hydrogen peroxide, which can promote oxidative damage throughout the cell. It has been well documented that high levels of reactive oxygen species (ROS) are consistently associated with the activation of pro-apoptotic pathways (Giorgio et al., 2005; Sideris & Tokatlidis, 2010). Therefore, when studying aging at a cellular level, processes that potentially promote ROS formation are of particular interest.

1.2 Reactive Oxygen Species

ROS consist of radical and non-radical oxygen species such as superoxide anion (O_2^-), hydrogen peroxide (H_2O_2) and hydrogen radical ($HO\bullet$) (Ray, Huang, &

Tsuji, 2012). ROS are derived intracellularly from three main sources and serve a multitude of different purposes based on its levels. Two sources of ROS occur at the cytoplasmic membrane and are created by NADPH oxidases (NOXs) and 5-lipoxygenase. NOXs promote ROS formation in the cytoplasm when stimulated by integrins, cytokines, oncogenic Ras, and growth factors (Novo & Parola, 2008). NOXs create ROS during the metabolism of NADPH to $\text{NADP}^+ + \text{H}^+$ and the coupling of extracellular oxygen radicals with H^+ molecules. In a similar manner, 5-lipoxygenase creates ROS through the creation of hydroperoxyeicosatetraenoic acid (HPETE) in a Ras dependent manner (Novo & Parola, 2008). The third and arguably most proficient source of intracellular ROS occurs from the mitochondria (Sena & Chandel, 2012).

Mitochondrial derived ROS occur naturally as a by-product of oxidative phosphorylation, where oxygen is metabolized in a co-ordinated manner with the Krebs cycle to generate adenosine triphosphate (ATP) (Sena & Chandel, 2012). Mitochondrial derived ROS are considered the main source of intracellular ROS because oxidative phosphorylation is occurring constantly. The function of the ETC is to couple electron transfer between electron donors (NADH) and acceptors (O_2), to the transfer of hydrogen ions across the inner mitochondrial membrane (through complex 1-4), thereby converting molecular oxygen (O_2) to water (H_2O) (Beckman & Ames, 1998). The resulting electrochemical gradient is utilized to generate energy in the form of ATP. The four ETC complexes along with cytochrome c channel electrons during oxidative phosphorylation to assist in the formation of water, however each electron exchange allows for potential electron leakage (Beckman & Ames, 1998).

To combat electron leakage, cells produce ROS scavenging proteins such as peroxidases, thioredoxins (TRXs), peroxiredoxins (PRXs), superoxide dismutases (SODs) and other anti-oxidants located both in the mitochondria (i.e. PRXIII, MnSOD) and cytosol (i.e. Catalase, PRXI, TRX, SOD1) (Gertz, Fischer, Wolters, & Steegborn, 2008; Nemoto & Finkel, 2002). These proteins function to detoxify high levels of ROS, while allowing a certain level of ROS to persist for various regulatory and signaling events (Nemoto & Finkel, 2002). However specific mechanisms controlling the physiological production of ROS, and the downstream signaling events affected by these oxidants, are poorly understood.

1.3 Shc Protein Family and the p66Shc isoform

The Src homologous and collagen-like (Shc) family of proteins are generally characterized as adaptor proteins that participate in receptor tyrosine kinase-dependent activation of Ras in the cytoplasm (Rety et al., 1996). There are three main isoforms of Shc, each named in accordance to weight; p46Shc (46 kDa), p52Shc (52 kDa) and p66Shc (66 kDa) (Pelicci et al., 1992). Each Shc isoform is transcribed from the *ShcA* locus (mammals) where each Shc isoform is transcribed and differentially spliced (Wills & Jones, 2012). While p46Shc and p52Shc function as adaptor proteins for the Grb2 complex and activation of the Ras signaling pathway, p66Shc has been shown to inhibit activation of the Ras/MAPkinase pathway triggered by the EGF and IGF-1 receptors (Trinei et al., 2009). This evidence suggests Shc proteins maintain a balanced equilibrium in regards to Ras pathway activity (Nemoto et al., 2006).

Common to all three Shc isoforms is a collagen homology domain (CH1) enriched in proline and glycine, a phosphotyrosine binding domain (PTB) and a Src homologous type 2 domain (SH2) at the C-terminus (Trinei et al., 2009). Unique to p66Shc is an additional collagen homology domain (CH2) at the N-terminus of the protein, which is not present in either the p46Shc or p52Shc isoforms. The Shc isoform p66Shc has been shown to serve multiple functions depending on its phosphorylation status and localization (Trinei et al., 2009). p66Shc is a protein that promotes increased intracellular ROS production and affects longevity in mice (Di Lisa, Kaludercic, Carpi, Menabo, & Giorgio, 2009). Previous research using p66Shc knockout mice (-/-) have shown significantly decreased intracellular ROS levels and increased longevity of up to 30% compared to control wild-type mice (Migliaccio et al., 1999). Following exposure to cellular stress (i.e. H₂O₂ or UV), the p66Shc isoform has been shown to translocate into the intermembrane space (IMS) of mitochondria (Pinton & Rizzuto, 2008). The additional CH2 domain found in the p66Shc is necessary for its translocation into the mitochondria; an event necessary for increased ROS production (Gertz et al., 2008). Protein Kinase C- β (PKC- β) actively phosphorylates p66Shc at serine position 36 in response to a cellular stress. Serine phosphorylation at position 36 ultimately promotes association with Pin1, subsequent isomerization of a phosphor-Ser36-Pro37 bond and initiates the mitochondrial translocation event (Gertz et al., 2008; Pinton & Rizzuto, 2008).

Once present in the mitochondria, the specific physical activity of p66Shc is relatively unclear, however p66Shc has been shown to increase mitochondrial ROS by directly increasing ROS production, and also impairing ROS response mechanisms

(Nemoto & Finkel, 2002). Expression and activity of the ROS scavenger Mitochondrial Superoxide Dismutase (MnSOD) is impaired by p66Shc (Pani, Koch, & Galeotti, 2009). The subsequent increase of ROS can diffuse into the cytosol and inactivate FOXO transcription factors through phosphorylation by the AKT pathway (Song, Ouyang, & Bao, 2005). FOXO transcription factors induce MnSOD and catalase activity, therefore p66Shc mediated repression of MnSOD activity combined with inactivation of FOXO transcription factors within the cytosol by diffused ROS creates a positive feed-forward loop amplifying the oxidative cascade created by p66Shc (Pani et al., 2009).

Upon translocation into the mitochondrial IMS, p66Shc promotes the formation of mitochondrial ROS through direct/indirect interactions with the ETC (Giorgio et al., 2005). Within the IMS, p66Shc is suggested to mediate electron transfer from cytochrome c to oxygen, by virtue of its cytochrome c binding domain, and promote increased $O_2^{\bullet-}$ formation. $O_2^{\bullet-}$ is subsequently converted to hydrogen peroxide (H_2O_2) by SOD1. The physical accumulation of p66Shc and associated H_2O_2 production within the IMS could potentially upset the balance of redox sensitive proteins involved in electron transport and ROS maintenance. Furthermore, the presence of p66Shc within the IMS could catalyze widespread changes to the disulfide proteome within the mitochondria and initiate a stress response, opening of a mitochondrial permeability transition pore and the release of apoptotic factors into the cytosol (Sideris & Tokatlidis, 2010; Sohal & Orr, 2012). The increased levels of membrane permeable H_2O_2 associated with p66Shc localization to the mitochondria may also affect redox sensitive proteins located further downstream within the cytosol, leading to widespread changes in the cytoplasmic disulfide proteome (Figure 1) (Cumming et al., 2004). Therefore, assessing the disulfide

proteome of the mitochondria and cytosol individually may help elucidate the precise function of p66Shc.

1.4 Regulatory Mechanisms of Protein Disulfide Bonds

Recent studies have shown that changes in protein DSBs can affect cell signaling with some specificity (Gertz et al., 2008). The importance of protein disulfide bonds was first noted in 1961 by Anfinsen and Haber, which helped illustrate the importance of DSBs for protein stability and function (Anfinsen & Haber, 1961). Disulfide bond formation predominantly occurs in the oxidizing environment of the endoplasmic reticulum, which permits the formation of DSBs in a controlled manner (Cumming et al., 2004). Most protein cysteine residues have a $pK_a > 8.0$, causing them to remain protonated in reducing environments, such as the cytoplasm and nucleus. However, there is a small group of redox-sensitive proteins, which contain cysteine amino acid residues that exist as thiolate anions (Cys-S⁻) at physiological pH (7.2 pKa). This occurs as a result of a lowering of pKa values by charge interactions with neighbouring amino acid residues (Cumming et al., 2004). Cysteine residues that exist as thiolate anions at physiological pH have been found to undergo disulfide bonding in the cytosol and nucleus under both oxidative and non-oxidative conditions (Cumming et al., 2004). Various proteins can promote DSB formation such as redox-dependent receptors (Mia40) and sulfhydryl oxidases (Erv1) (Sideris & Tokatlidis, 2010). Both Mia40 and Erv1 are present in the mitochondrial IMS and research has suggested their involvement in DSB formation during the potentially oxidizing conditions of the mitochondrial environment (Nemoto & Finkel, 2002; Sideris & Tokatlidis, 2010).

Numerous proteins have recently been identified as undergoing reversible protein DSB formation as a regulatory mechanism (Gertz et al., 2008). Proteins such as the proto-oncogene tyrosine-protein kinase Src and other tyrosine kinases can be inactivated by ROS induced disulfide bonding (Cys-S-S-Cys) (Inaba, 2010; Rety et al., 1996). Well-characterized redox sensitive proteins like Src exhibit changes in activity related to DSB formation and possess conserved sequences that are shared among homologous proteins (Gertz et al., 2008). It stands to reason that conserved sequences within a redox sensitive protein shared among multiple proteins may provide clues about the redox-regulated activity of those protein families. For the purposes of the research described here, p66Shc and its influence on the disulfide proteome is of particular interest.

Disulfide bonding of p66Shc may allow translocation of the protein into the mitochondria by altering its conformation. Once translocated into the mitochondrial IMS, p66Shc is believed to promote ROS formation, possibly through inter- or intra-molecular DSB interactions with native proteins (Pinton & Rizzuto, 2008). The exact activity of p66Shc within the mitochondrial IMS has yet to be conclusively determined, however the well documented increase in mitochondrial ROS production associated with p66Shc mitochondrial translocation may lead to indirect changes to the disulfide proteome in other cellular compartments. Similarly, proteins within the cytosol and other subcellular locations can be affected by ROS-induced formation of disulfide bonds within kinases, phosphatases, antioxidant proteins and structural proteins (Paulsen & Carroll, 2010). Changes identified in these downstream proteins may provide clues about how p66Shc expression affects cellular longevity.

1.5 Cell Stress Responses and Rationale

A number of studies have provided valuable evidence concerning the detrimental role of increased H_2O_2 production and the potential downstream effects of p66Shc-mediated ROS on protein phosphorylation and gene expression (Carpi et al., 2009). p66Shc mediated ROS production can affect cells by triggering either cell survival responses, cell stress responses or potentially apoptotic responses (Migliaccio et al., 1999). The particular defense system a cell mounts against increased cellular stress depends heavily on the best chance for survival (Fulda, Gorman, Hori, & Samali, 2010). There are several known stress response mechanisms and pathways such as heat shock response, unfolded protein response and DNA damage response. These responses function to regulate cell death in response to cell injuries administered by specific stresses (Samali, Fulda, Gorman, Hori, & Srinivasula, 2010). However, the increase in p66Shc mediated ROS associated with p66Shc serine phosphorylation has been suggested to activate an oxidative stress response (Fulda et al., 2010).

Previous studies suggest a close relationship between increased intracellular ROS levels and apoptosis (Fulda et al., 2010; Sohal & Orr, 2012). Upon recognition of rising ROS levels, or following a disruption in the ability to reduce ROS levels, an oxidative stress response is initiated for cell survival (Rabilloud, Chevallet, Luche, & Leize-Wagner, 2005). As previously stated, a main contributor of intracellular ROS production occurs through inefficient electron transport from the ETC. However, the exact site of ROS production may not be as important for initiating a stress response but rather redox specific signaling further downstream may trigger a stress response (Sohal & Orr, 2012).

Situations where high levels of ROS are produced generally lead to loss of mitochondrial membrane potential ($\Delta\Psi_m$), the release of cytochrome C from the mitochondria to the cytosol and activation of the apoptotic pathway (Di Lisa et al., 2009). Apoptosis triggered by mitochondrial-derived ROS may be regulated by any number of stress receptors, potentially located in the mitochondria, nucleus or cytosol (Fulda et al., 2010; Sato et al., 2009). Therefore it is imperative to examine redox modifications of proteins in different subcellular locations. Specifically, comparing alterations in the DSB status of mitochondrial versus cytosolic proteins may provide better clues to downstream effectors of p66Shc-signaling.

1.6 Hypothesis and Research Outline

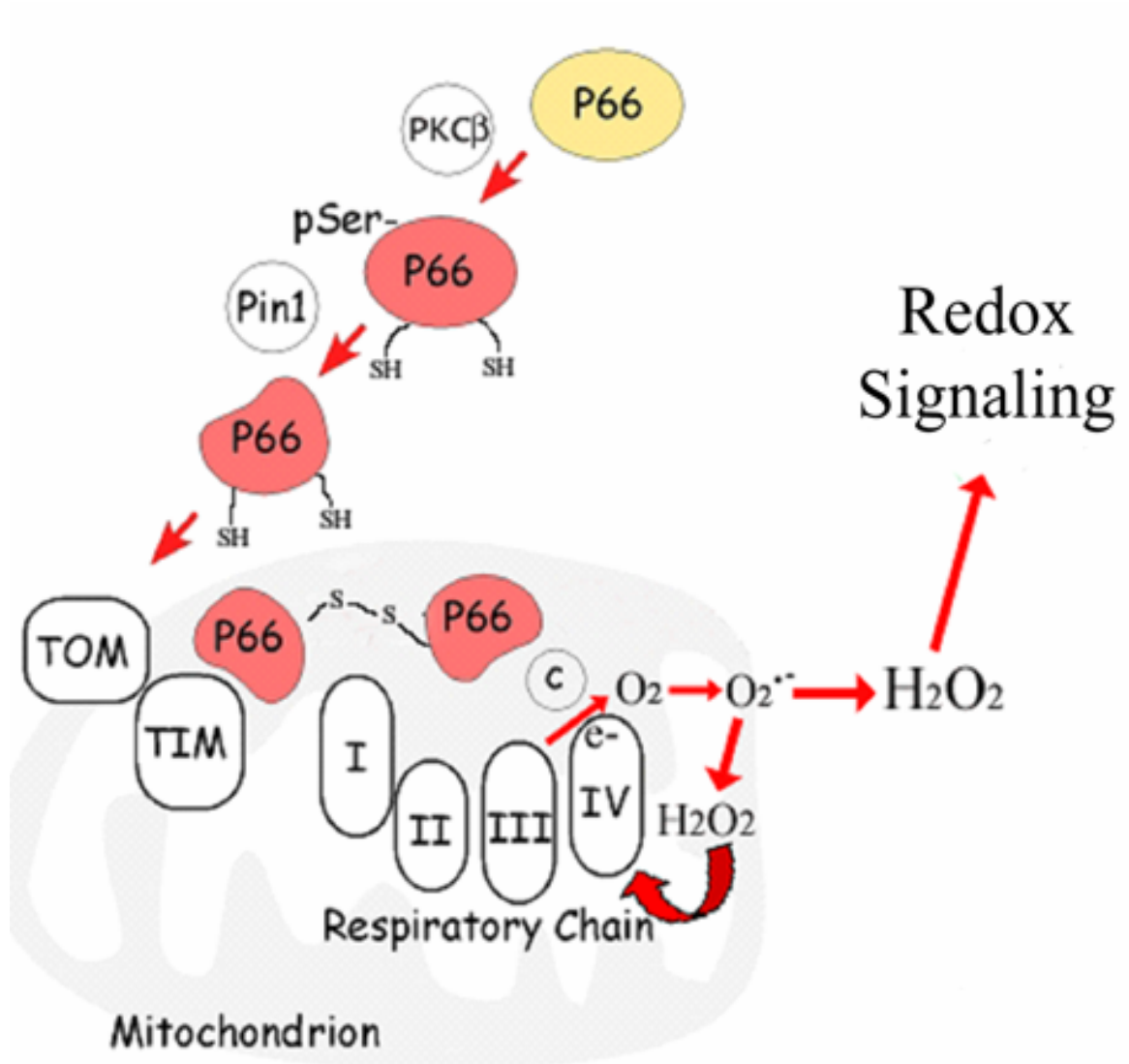
I hypothesize that ectopic expression and chemical activation of p66Shc in the mouse hippocampal cell line (HT-22) will promote increased mitochondrial ROS production and lead to altered disulfide bonding of proteins within the mitochondrial and cytosolic compartments. Changes in disulfide bonding of specific proteins may mediate some of the downstream signaling events associated with p66Shc activation.

By expressing an HA-tagged p66Shc expression vector in HT-22 cells, this research intends to assess the effects of p66Shc activation on the disulfide proteome within mitochondrial and cytosolic subcellular compartments. A PKC- β agonist (DOPPA) will be used to induce serine-36 phosphorylation of p66Shc, promoting its translocation into the mitochondria. Experiments will be performed to determine if ectopic p66Shc expression and DOPPA induced serine phosphorylation will (a) produce

increased ROS levels and lead to decreased cell viability and (b) alter the disulfide proteome of mitochondrial and cytosolic fractions compared to control (pcDNA) transfected cells following analysis by two-dimensional (2D) redox polyacrylamide gel electrophoresis (PAGE) analysis. Disulfide bonded proteins (DSBPs) reproducibly affected by p66Shc activation will be identified by mass spectrometry. This research aims to establish the effects of p66Shc expression and serine phosphorylation on the disulfide proteome within the mitochondrial and cytosolic compartments. Alterations detected in the subcellular disulfide proteome may reveal novel mechanisms of p66Shc stress response activation and initiation of apoptotic pathways.

Figure 1. Model of p66Shc mediated mitochondrial ROS production. Under control conditions, p66Shc localizes to the plasma membrane until cellular stress triggers PKC- β activation and phosphorylation of p66Shc on the serine amino acid residue located at position 36 within the CH2 domain. This phosphorylation event causes peptidyl-prolyl cis-trans isomerase NIMA-interacting 1 (Pin1) to associate and promote isomerization of a phosphor-Ser36-Pro37 bond in p66Shc thereby allowing it to translocate into the mitochondrial intermembrane space (IMS). The role of p66Shc within the mitochondrial IMS is poorly defined, however it is believed that p66Shc mediates electron transfer from cytochrome C to oxygen by virtue of its cytochrome C binding domain and promotes increased superoxide (O_2^-) formation. O_2^- is converted to hydrogen peroxide (H_2O_2) by SOD1. Increased mitochondrial H_2O_2 may oxidize proteins within the mitochondrial IMS that may be associated with electron transport during oxidative phosphorylation, further accelerating the release of oxygen radicals as part of a positive forward-feed loop mechanism. H_2O_2 may also diffuse into the cytosolic domain of the cell and initiate changes to redox-sensitive proteins which participate in signaling processes. Note: Adapted from “p66Shc Signals to Age” (Trinei et al., 2009).

Figure 1



Chapter 2

Materials and Methods

2.1 Cell Culture Conditions

The immortalized mouse hippocampal cell line HT-22 was provided by Dr. David Schubert, The Salk Institute, LaJolla, CA. HT-22 cells were chosen because they are neuronal in origin, and many studies have suggested mitochondrial dysfunction and increased ROS levels in the CNS correlates with aging and neurodegeneration (Beckman & Ames, 1998; Su et al. 2012). Cells were cultured in Dulbecco's Modified Eagles Medium (DMEM) supplemented with 10% fetal bovine serum (FBS) and 1% penicillin/streptomycin. Cells were incubated at 37°C in a CO₂ incubator with 5% CO₂/95% humidified air atmosphere and maintained at a maximum density of no more than 85% confluency.

2.2 HA-tagged p66Shc Vector Construction

A human pcDNA-p66Shc wild-type vector template was generously provided by Dr. Mauro Cozzolino, Fondazione Santa Lucia IRCSS, Rome, Italy. The p66Shc expression construct was sequenced (DNA Sequencing Facility, Robarts Research Institute, London, Ontario) to determine accuracy of the sequence before proceeding with further molecular work. Once p66Shc sequence accuracy was determined, the p66Shc vector was used as a template to create and amplify a HA-tagged p66Shc isoform using a Polymerase Chain Reaction (PCR)-based strategy (Invitrogen, Burlington, Ontario, Canada) supplemented with Dimethyl Sulfoxide (DMSO) to inhibit the formation of secondary or tertiary structures during the reaction. The forward primer sequence was 5'-

GACGATAGTCCGACTACCCTGTGT – 3' and the reverse primer sequence was 5' – ACTCTAGATTAAGCGTAGTCTGGGACGTCGTATGGGTACAGTTTCCGCTCCAC AGG – 3'. The amplified HA-tagged p66Shc sequence was then digested using the restriction enzymes EcoRI and XbaI (Invitrogen Canada) as these restriction sites had been incorporated into the 5' and 3' PCR primers respectively. The digested PCR product was then ligated into a pcDNA3.1 vector previously digested with EcoRI and XbaI and incorporation of the PCR product was confirmed by sequencing (Robarts DNA Sequencing Lab, London, Ontario, Canada).

2.3 Transfection and activation of HA-tagged p66Shc

Depending on the requirements of the experiment, HT-22 cells were seeded at 5×10^5 in a 100 mm cell culture dish or 3×10^5 in a 60 mm cell culture dish (BD Biosciences Canada). Cells were transiently transfected with either an empty pcDNA3.1 vector (control) or the p66Shc-HA expression plasmid. Briefly, 5 μ g p66Shc-HA DNA was combined with 8 μ l of Lipofectamine 2000 (Invitrogen) in 1 mL of Opti-MEM transfection media (Invitrogen) and added to HT22 cells then placed in a 37°C CO₂ incubator (5% CO₂, 95% O₂) for 5 hours. In a pilot experiment, transfection efficiency was confirmed by co-transfecting pGFP with p66Shc (1:3 ratio), to ensure that at least 50% of the cells were expressing GFP. p66Shc requires phosphorylation at the serine amino acid residue located at position 36 by PKC- β to become activated (Trinei et al., 2009). This phosphorylation event occurs following exposure to stressors such as H₂O₂ or UV light. However, taking into consideration that introducing HT-22 cells to those types of stresses may cause changes to the disulfide proteome irrespective of p66Shc activation,

a more specific agonist of PKC- β was required. Previous studies have suggested that 12-deoxyphorbol 13-phenylacetate 20-acetate (DOPPA) (Sigma-Aldrich, Oakville, Ontario, Canada), a PKC- β agonist, may be able to initiate PKC- β in a much more specific manner than treatment with H₂O₂ or UV (Ryves, Evans, Olivier, Parker, & Evans, 1991). DOPPA is a phorbol ester that works in concert with diacylglycerol to activate PKC- β by disrupting the association of an inhibitory pseudosubstrate (Gschwendt, Kittstein & Marks, 1991). Empirical experimentation determined that a treatment of 50 nM DOPPA for 6 hours was the optimal concentration and exposure time for p66Shc-HA phosphorylation (Figure 3A and B). Following transfection, cells were placed back in serum supplemented DMEM where they remained untreated (control) or exposed to 50 nM DOPPA for 6 or 12 hours as required.

2.4 Conventional SDS PAGE and Immunoblot Analysis

Once transfection and appropriate treatment was completed, cells were washed using Phosphate Buffered Saline (PBS) (VWR Canada), then harvested using a 1% Triton-X lysis buffer (50 mM Tris pH 7.5 (Sigma-Aldrich), 1% Triton-X (Sigma-Aldrich), 40 mM Iodoacetimide (IA) (Sigma-Aldrich), 1mM phenylmethanesulfonylfluoride (Sigma-Aldrich), 50 mM Sodium Fluoride (NaF) (Sigma-Aldrich) and 10mM Sodium Orthovanodate (Na₃VO₄) (Sigma-Adrich). Protein concentrations of the lysates were quantified using a colourimetric DC Protein Assay Kit (BioRad, Hercules CA).

Protein extracts (20-30 μ g) were reduced in loading buffer containing 100 mM dithiothreitol (DTT) and 2% beta mercaptoethanol (BME), boiled and resolved by SDS-

PAGE (12%) using a Mini-PROTEAN electrophoresis apparatus (BioRad Canada, Mississauga, ON). Proteins were then transferred from the gel onto polyvinylidene fluoride (PVDF) membrane (Millipore, Bedford, MA) by electroblotting, and blocked with 2% bovine serum albumin and 2% milk in tris-buffered saline with Tween-20, pH 7.5 (TBS-T). Membranes were then probed with one of the following antibodies: mouse Anti-Total Shc (BD Transduction Laboratories, Mississauga, ON), monoclonal mouse Anti β -actin (Sigma-Aldrich), mouse anti-Phosphorylated-p66Shc (Calbiochem, San Diego, CA), mouse anti-Voltage Dependent Anion Channel (VDAC) (Cell Signaling, Danvers MA), monoclonal mouse anti-HA (Covance, Berkeley, California) and anti tropomyosin-3 (Genetex, Irvine, CA).

After overnight incubation, membranes were washed for 3 x 10 minutes in TBS-T and incubated in goat-anti-mouse horseradish-peroxidase conjugated secondary antibody (Jackson ImmunoResearch, West Grove, PA) for 2 hours. Following incubation, membranes were again washed 3 x 10 minutes in TBS-T, and developed using Pierce ECL Western blotting reagents (Thermoscientific, Waltham, MA), and protein signal was detected using a ChemiDoc digital imaging system (BioRad Canada).

2.5 Mitochondrial ROS analysis

To measure mitochondrial ROS production, cells were seeded at a density of 1×10^5 cells in six 35 mm plates. After 24 hours, cells on three of the plates were transiently transfected with an empty pcDNA3.1 expression vector, and the other three were transiently transfected with the p66Shc-HA overexpression construct. Each pair of transfected cells (i.e. one pcDNA3.1 and one p66Shc-HA per pair) were subjected to

varying time lengths of 50 nM DOPPA exposure (No treatment, 6 hours, 12 hours) to determine optimal changes in mitochondrial ROS levels. After transfection and appropriate treatment, media was replaced with serum-free DMEM containing 200 nM MitoTracker® Red CM-H2XRos (Invitrogen Canada) and incubated for 30 min. Cells were then washed twice with warm phenol red-free DMEM, followed by incubation in phenol red-free DMEM with 10 µg/ml Hoechst (Sigma-Aldrich) for 3 minutes at 37°C to stain for nuclei. Cells were then washed again in phenol red-free DMEM and visualized using a fluorescent microscope (Zeiss AxioObserver, 40X objective). Four images from randomly selected regions were taken from each different treatment using a Q Imaging camera and Q Capture Pro Software. The fluorescent intensity of each image was later quantified using Image J software. Images of MitoTracker® Red CM-H2XRos stained cells and Hoechst stained nuclei were merged to create figures.

2.6 Trypan Blue Exclusion Test

The effects of p66Shc-HA overexpression on HT-22 cell viability were determined using a trypan blue (VWR Canada) dye exclusion test. HT-22 cells were seeded at a density of 1×10^4 in triplicate in 2 – 12 well dishes. Cells were then transiently transfected with either 0.5 µg pcDNA3.1 (control) or 0.5 µg p66Shc-HA for 5 hours using Lipofectamine 2000 (Invitrogen Canada). After 5 hours, Opti-MEM media was replaced with the serum supplemented DMEM media. After 24 hours, cells were treated with DOPPA (50 nM) in DMEM and incubated for 6, 12 or 24 hours. At the end of each treatment, cells were collected using 100 µl of TrypLE Express (Invitrogen Canada) and incubated for 5 min at 37°C. Once the cells had detached, 100 µl of Trypan

Blue was added to the appropriate well, mixed, and loaded into a haemocytometer for counting. Cells that excluded trypan blue staining were counted as viable cells. Cell viability was calculated as a percentage based on the number of viable cells versus total number of cells in each treatment.

2.7 HT-22 Subcellular Fractionation and Mitochondrial Isolation

For each experimental treatment (pcDNA3.1, p66Shc-HA, pcDNA3.1+DOPPA (50 nM), p66Shc-HA+DOPPA (50 nM)) cells were seeded on eight 100 mm plates at a density of 5×10^5 cells per plate. Cells were transiently transfected as previously described and half the cells were treated with DOPPA (50 nM) for 12 hours. Cells were then centrifuged at $400 \times g$ for 5 min, washed and resuspended using 1 ml warm PBS, then transferred to a 1.5 ml microfuge tube (VWR Canada) and pelleted again. A mitochondrial isolation kit (ThermoScientific, Waltham, MA) was used to fractionate the mitochondria using a series of kit-specific buffers and centrifuge spins according to the manufacturer's instructions. Once cytosolic and mitochondrial fractions were isolated, a 1% Triton-X lysis buffer was added to the mitochondrial fraction, and lysed mechanically by repeatedly pipetting the solution rapidly. Cytosolic and mitochondrial fractions were then prepared accordingly for either redox 2-D PAGE or reduced/non-reduced 1-D PAGE analysis.

2.8 Redox 2D SDS PAGE Analysis

Protein extracts from subcellular fractions were quantified by a colorimetric DC Protein Assay Kit (BioRad). Once quantified, protein samples (150 – 200 μ g of Triton-X

lysate) were resolved through a 1.5 mm, 12% acrylamide gel for 16 hours at constant current. Gel strips were then cut and soaked in a SDS loading buffer (0.5M Tris-HCl, 5% glycerol, 2% SDS) containing 100 mM DTT for 20 min at room temperature. The gel strips were then rinsed twice with SDS running buffer and soaked in SDS loading buffer containing 40 mM IA for 10 min at room temperature to alkylate newly exposed thiol groups. Gel strips were then rinsed again 2 X in SDS running buffer and individual lanes containing each protein samples were cut to a width of approximately 5 mm wide then loaded horizontally into a second 1.5 mm, 12 % acrylamide gel and resolved for 16 hours at constant current. The resulting 2D gels were then fixed in 50% methanol overnight.

2.9 Silver Staining of Redox 2D Gels

Following methanol fixation, the gels were washed 3 X 20 min in H₂O, and then sensitized in 0.02% sodium thiosulfate for 90 sec, immediately followed by 3 X 30 sec washes in H₂O. Gels were then stained with 0.1% silver nitrate for 30 min at room temperature, washed 3 X 1 min in H₂O and developed in 2% sodium carbonate, 0.0185% formaldehyde, and 0.0004% sodium thiosulfate. Gels were developed for approximately 10 min or until appropriate stain intensity was reached. Stain development was stopped using 6% acetic acid. Gels were then analyzed, and experimental gels (p66Shc-HA transfected) were compared to control gels to establish visual changes in DSBPs.

2.10 Identification of Redox Sensitive Proteins

DSBPs that were altered in a p66Shc-dependent manner were picked with an automated spot picker and digested in-gel using a MassPREP automated digester station

(ParkinElmer, Waltham MA). Silver stained gel pieces were de-stained using a 50 mM sodium thiosulfate and 15 mM potassium ferricyanide solution, followed by protein reduction using 10 mM DTT, alkylation using 55 mM IA, and tryptic digestion. Peptide extraction was completed using a formic acid (1%), acetonitrile (2%) solution, after which peptides were lyophilized. Peptide samples were then re-dissolved in a 10% acetonitrile, 0.1% trifluoroacetic acid solution, and then mixed 1:1 (v/v) with MALDI matrix (α -cyano-4-hydroxycinnamic acid), prepared as 5 mg/mL in 6 mM ammonium phosphate monobasic, 50% acetonitrile, 0.1% trifluoroacetic acid). Digested protein samples were identified using a 4700 Proteomics Analyzer MALDI TOF (Applied Biosystems, Foster City, CA) equipped with a 355 nm Nd:YAG laser. Data acquisition and processing were accomplished using the 4000 Series Explorer and Data Explorer, respectively (both from Applied Biosystems). Reflection (positive and negative) ion mode was used and the instrument was calibrated at 50 ppm mass tolerance, with each mass spectrum collected as a sum of 1000 shots. Identities of the isolated disulfide linked proteins were determined through NCBI rodent (*Mus musculus*) protein database searches.

2.11 TRITC-Phalloidin Immunostaining of Actin Filaments

In a 12 well dish, cells were seeded at a density of 1×10^5 on coverslips that had previously been treated with polylysine (Invitrogen Canada) to ensure proper cell adherence. After 24 hours, media was removed and cells were transiently transfected with pcDNA3.1 (control) and p66Shc-HA using Opti-MEM media and Lipofectamine for 5 hours as previously described. Following transfection, the Opti-MEM media was

aspirated and serum supplemented DMEM containing 50 nM DOPPA was added to designated wells for a 6 or 12 hour treatment. Upon completion of DOPPA treatment, each well was aspirated and washed 2 X with 37°C PBS, then fixed in 4% Paraformaldehyde in PBS for 10 min. Cells were then blocked using 1% BSA in PBS for 30 min to prevent any non-specific binding. Each coverslip was then stained with 30 μ l of TRITC-Phalloidin (5 μ g/ml in PBS with 1% BSA) for 20 min. Following TRITC-Phalloidin staining, nuclei were stained by incubating coverslips in 50 μ g/mL Hoescht 33342 (Sigma-Aldrich) for 3 min. Coverslips were then washed 2 X in cold PBS and mounted on slides using Prolong Gold Antifade mounting media (Invitrogen). Stained cells were visualized using a fluorescent microscope (Zeiss AxioObserver, 40X objective).

2.12 Nonreducing/Reducing 1D SDS PAGE

Samples used for nonreducing/reducing 1D SDS PAGE were collected as previously described for conventional 1D SDS PAGE analysis. However, half of the sample was allocated and prepared separately, such that it was not exposed to reducing agents (BME or DTT) and extra caution was taken to avoid heat, thereby preserving disulfide bonds. The other half of the original sample was exposed to reducing agents and boiled for 5 min. The samples were then resolved in a 12% acrylamide mini-gel (BioRad) and proteins transferred onto a PVDF membrane where they were further probed for specific proteins and visualized by a ChemiDoc digital imaging system (BioRad) as described above.

2.13 Statistical Analysis

Statistical analysis of MitoTracker® Red CM-H2XRos data measuring mitochondrial ROS and trypan blue exclusion test data measuring cell viability data was performed using One-way ANOVA analysis. Comparisons of ROS production and percentage cell viability were performed using Post-hoc TUKEY tests. *P*-values of <0.05 were considered to be significant.

Chapter 3

Results

3.1 Production and expression of HA-tagged p66Shc overexpression construct

A pcDNA3.1 expression vector containing wildtype non-tagged p66Shc cDNA was obtained and used as a template for the generation of a HA-tagged p66Shc expression insert using a PCR strategy. Upon completion of the p66Shc-HA expression construct, sequencing was performed to ensure that the p66Shc and HA tag sequences were correctly incorporated. HT-22 cells were transfected with the non-tagged and HA-tagged p66Shc expression constructs and whole cell extracts were analyzed by Western blotting using an antibody that recognizes all Shc isoforms (Figure 2). Cells transfected with the control pcDNA3.1 plasmid exhibited no detectable expression of endogenous p66Shc. Interestingly, cells transfected with the HA-tagged p66Shc plasmid exhibited the highest levels of ectopic expression compared to cells transfected with the non-tagged version. In addition, following the reprobing of the blot with an anti-HA antibody, a ~66 kDa band was detected only in cells transfected with the HA-tagged p66Shc-tagged vector.

3.2 Phosphorylation of p66Shc using the PKC- β agonist DOPPA

Cytosolic p66Shc requires an additional phosphorylation event at serine 36 to initiate mitochondrial translocation (Gertz et al., 2008). To achieve site-specific phosphorylation, a PKC- β agonist (DOPPA) was employed as PKC- β has been shown to trigger phosphorylation of serine-36 in p66Shc (Trinei et al., 2009). Optimal levels of p66Shc phosphorylation were determined following testing a range of DOPPA

concentrations for 24 hours, followed by a time-course experiment. Initial analysis indicated that 25 nM and 50 nM DOPPA concentrations induced optimal phosphorylation of p66Shc following a 24 hour time exposure (Figure 3a). Further analysis revealed that 6 hours of DOPPA exposure time produced the highest levels of phosphorylated p66Shc at both concentrations (25 and 50 nM) tested (Figure 3b). Thus, for all subsequent experiments, a 6 hour treatment with 50 nM DOPPA post-transfection was performed to ensure optimal p66Shc activation.

3.3 p66Shc Activation increases Mitochondrial ROS Production

Previous research using cells derived from p66Shc *-/-* mice revealed a significant decrease of intracellular ROS levels (Migliaccio et al., 1999). Therefore, it stands to reason that overexpressing p66Shc, and treating cells with a PKC- β agonist (DOPPA), should increase mitochondrial ROS levels. To examine changes in mitochondrial ROS production, control and treated cells were stained with MitoTracker® Red CM-H2XRos, a dye which localizes to mitochondria and fluoresces red in the presence of ROS. HT-22 cells transfected with p66Shc-HA and treated with DOPPA displayed increased mitochondrial ROS when compared to either untreated p66Shc-HA or pcDNA3.1 transfected cells (Figure 4A). Although previous data had suggested 6 hours of DOPPA treatment was effective for p66Shc phosphorylation, statistical analysis of mitochondrial ROS levels suggested the 6 hours of 50 nM DOPPA treatment was an insufficient time to significantly increase mitochondrial ROS levels (Figure 4A and 4B). However, 12 hour DOPPA time treatment did promote a significant ($P < 0.05$) increase in ROS production in

Figure 2. Analysis of endogenous and ectopically expressed p66Shc levels in HT-22 cells. HT-22 whole cell lysates were analyzed by Western blotting using a total Shc antibody (which recognizes all Shc isoforms) to compare endogenous (pcDNA) and ectopic (p66Shc, p66Shc-HA) expression of p66Shc. p66Shc (top band in center panel) was only detected in p66Shc and p66Shc-HA transfected cells. In addition, the blot was reprobed with an anti-HA specific antibody to specifically detect the HA-tagged p66Shc variant. An anti-Actin antibody was used as a loading control.

Figure 2

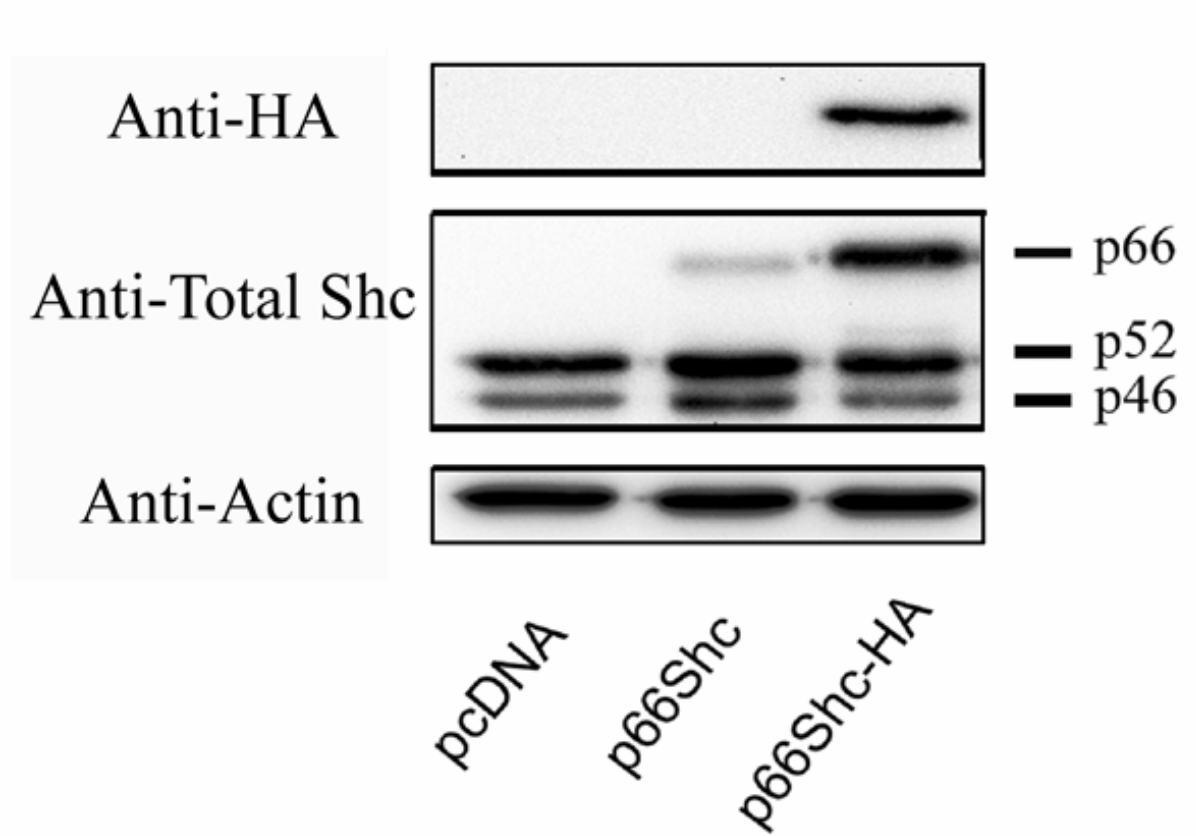


Figure 3. Optimization of p66Shc phosphorylation in HT-22 cells transfected with p66Shc expressing plasmids. (A) The effect of increasing concentrations of DOPPA (25, 50 and 100 nM) on p66Shc phosphorylation and expression levels over a 24 hour time period was assessed in pcDNA, p66Shc and p66Shc-HA transfected cells. (B) Time course of p66Shc expression and phosphorylation following DOPPA treatment (25 and 50 nM) over 2, 6 and 24 hours in control (pcDNA) and p66Shc-HA transfected HT-22 cells. Western blots were probed with antibodies that recognize serine-36 phosphorylated p66Shc (anti-P-Shc), all Shc isoforms (anti-TotalShc) and a loading control to ensure equal loading of protein samples across each treatment (anti-Actin).

Figure 3A

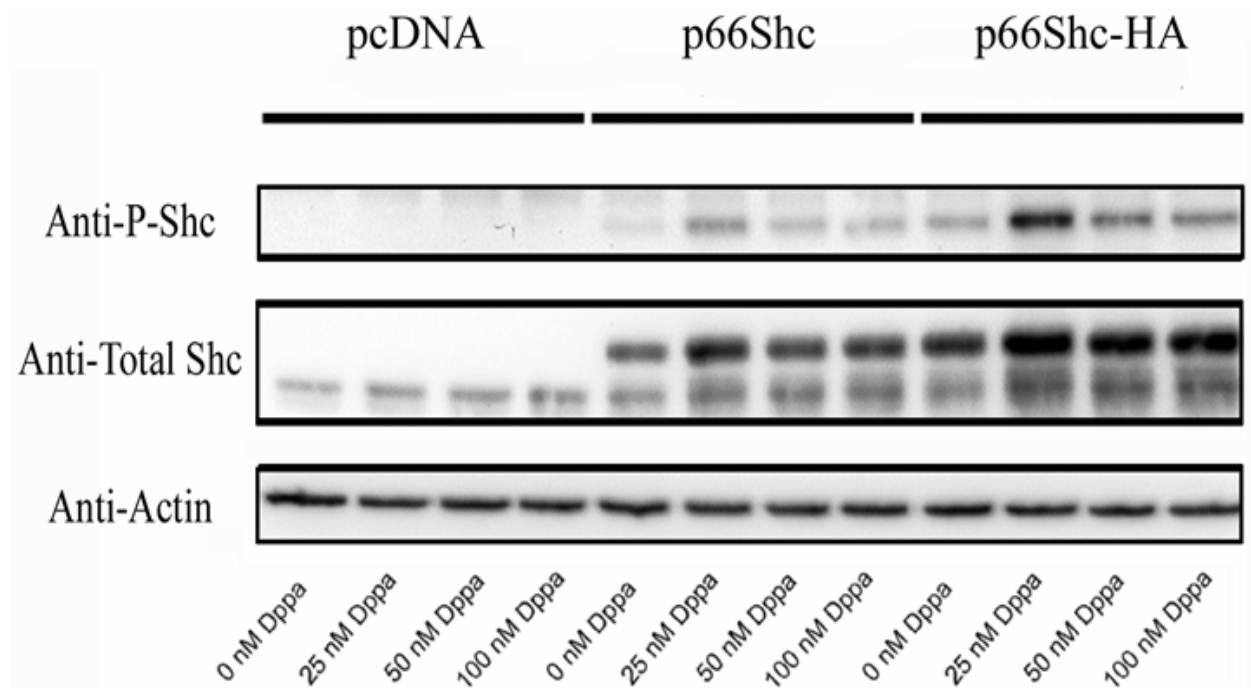
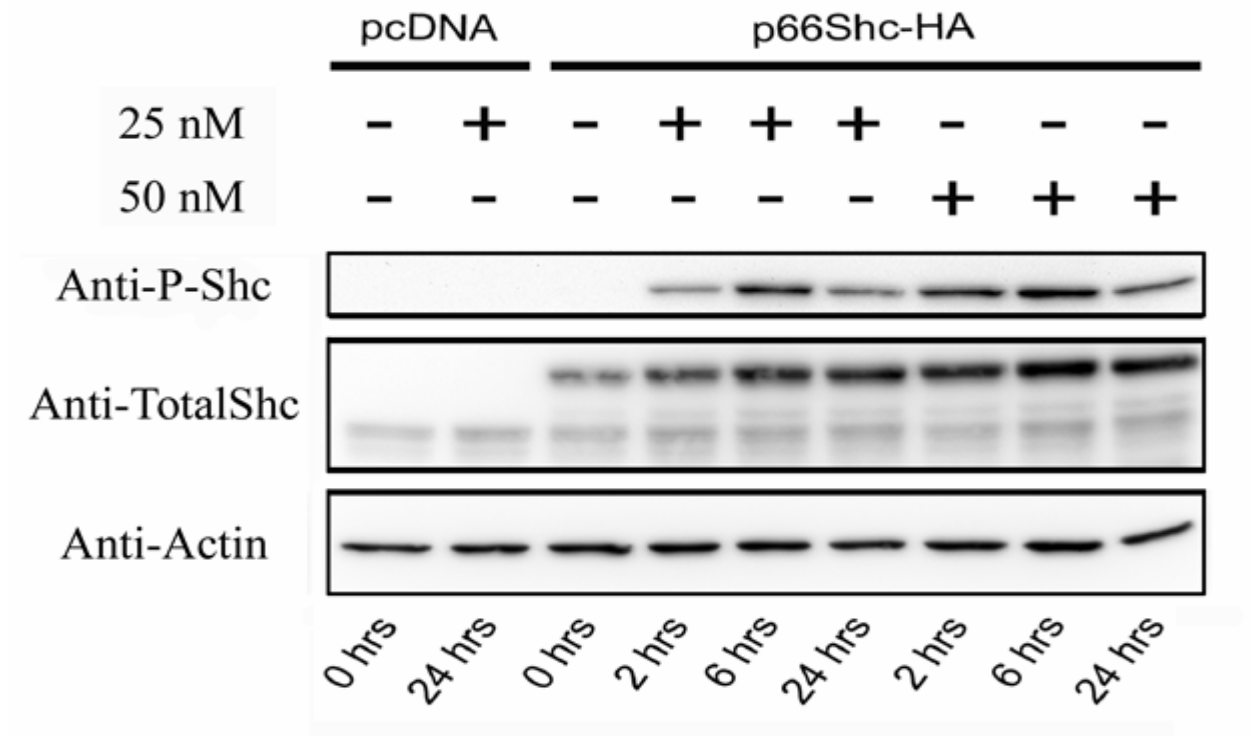


Figure 3B



p66Shc-HA transfected cells compared to control and p66Shc transfected (non-treated) cells at the same time point (Figure 4B).

3.4 p66Shc Activation Decreases Cell Viability

Studies have shown that knockout of the p66Shc gene increases longevity of mice by up to 30 percent, promoting both decreased ROS production and decreased cell death (Migliaccio et al., 1999). By this reasoning, overexpression of p66Shc should decrease cell viability after exposure to DOPPA in a time sensitive manner. A trypan blue exclusion test was performed to determine if p66Shc activation in HT-22 cells promotes decreased cell viability in accordance with other studies (Migliaccio et al., 1999). Indeed, HT-22 cell viability decreased significantly ($P < 0.05$) over time in cells transfected with p66Shc-HA and treated with DOPPA (50 nM) at 12 and 24 hours, but not in cells transfected with an empty pcDNA3.1 vector and treated similarly as determined by One-way ANOVA and Post-hoc TUKEY test (Figure 5). These results also revealed that DOPPA treatment for 12 hours provided the best timepoint for an increase in mitochondrial ROS production while the majority of cells still remained viable following p66Shc-HA activation.

Figure 4. Effect of p66Shc phosphorylation on mitochondrial ROS production in HT-22 cells. (A) Mitochondrial ROS levels (red fluorescence, as detected by MitoTracker® Red CM-H2XRos) in HT-22 cells transfected with pcDNA3.1 and p66Shc-HA plasmids and treated with 50 nM DOPPA for 6 and 12 hours. Nuclei were counterstained with Hoescht 33242 (blue fluorescence) and the two images were merged together. (B) MitoTracker® Red CM-H2XRos fluorescence was quantified using ImageJ software and statistically analyzed by One Way ANOVA and Post-hoc Tukey analysis. A significant increase (*, $P < 0.05$) in mitochondrial ROS production was observed in p66Shc-HA transfected cells following 12 hours of DOPPA treatment compared to untreated or control cells.

Figure4A

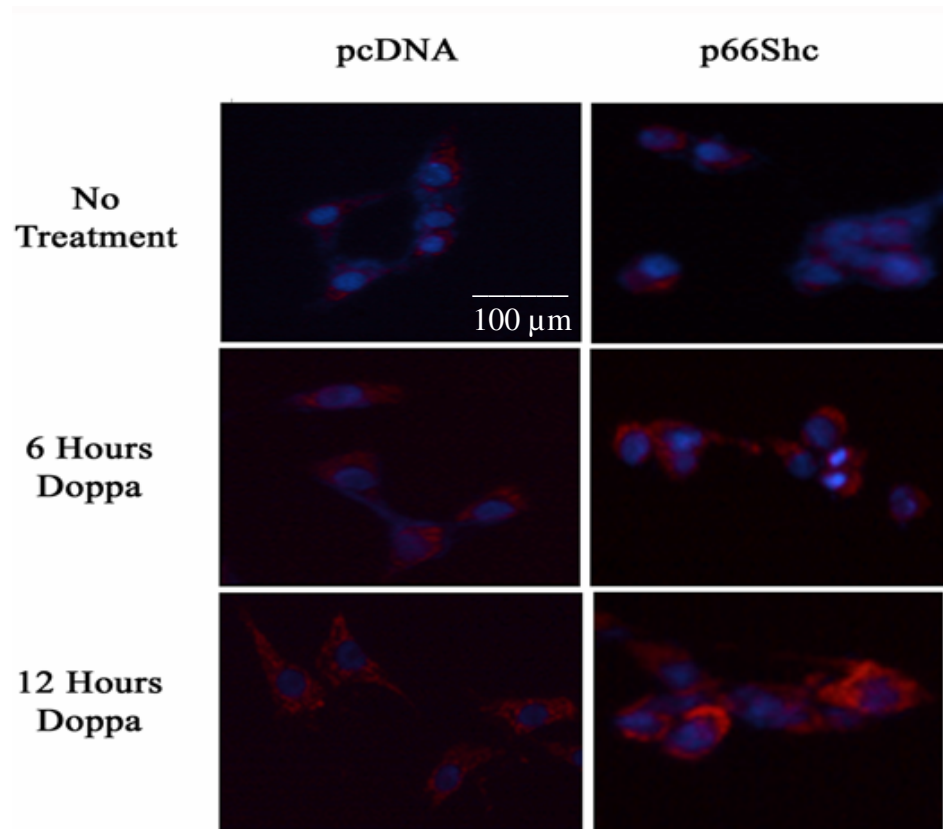


Figure4B

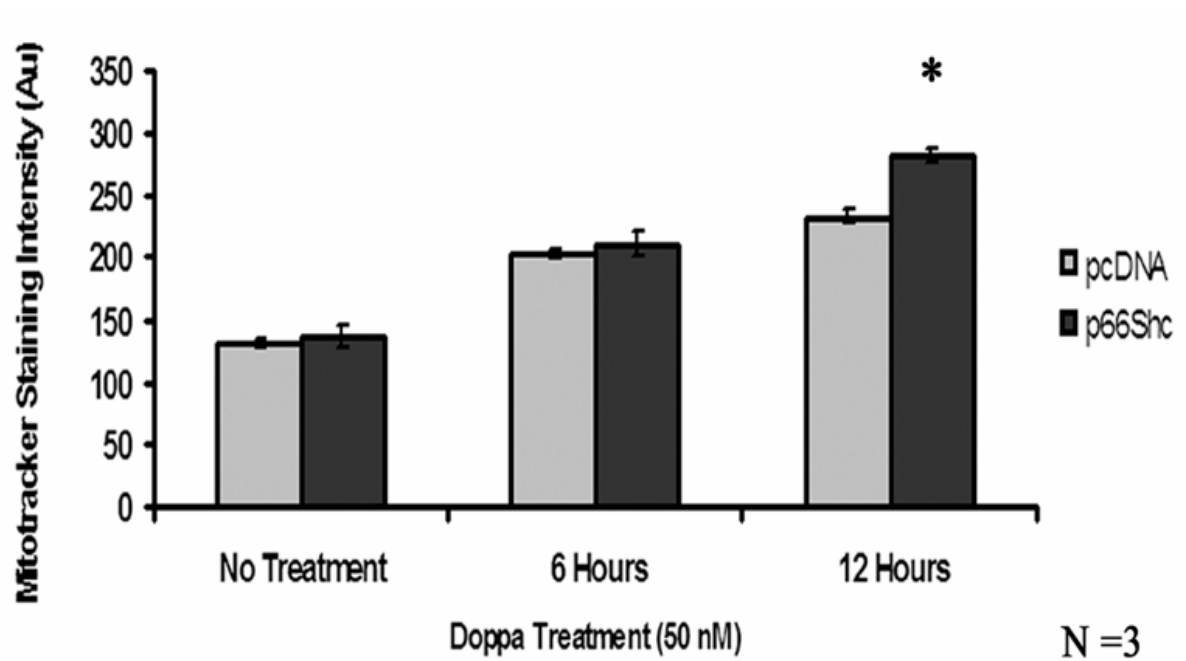
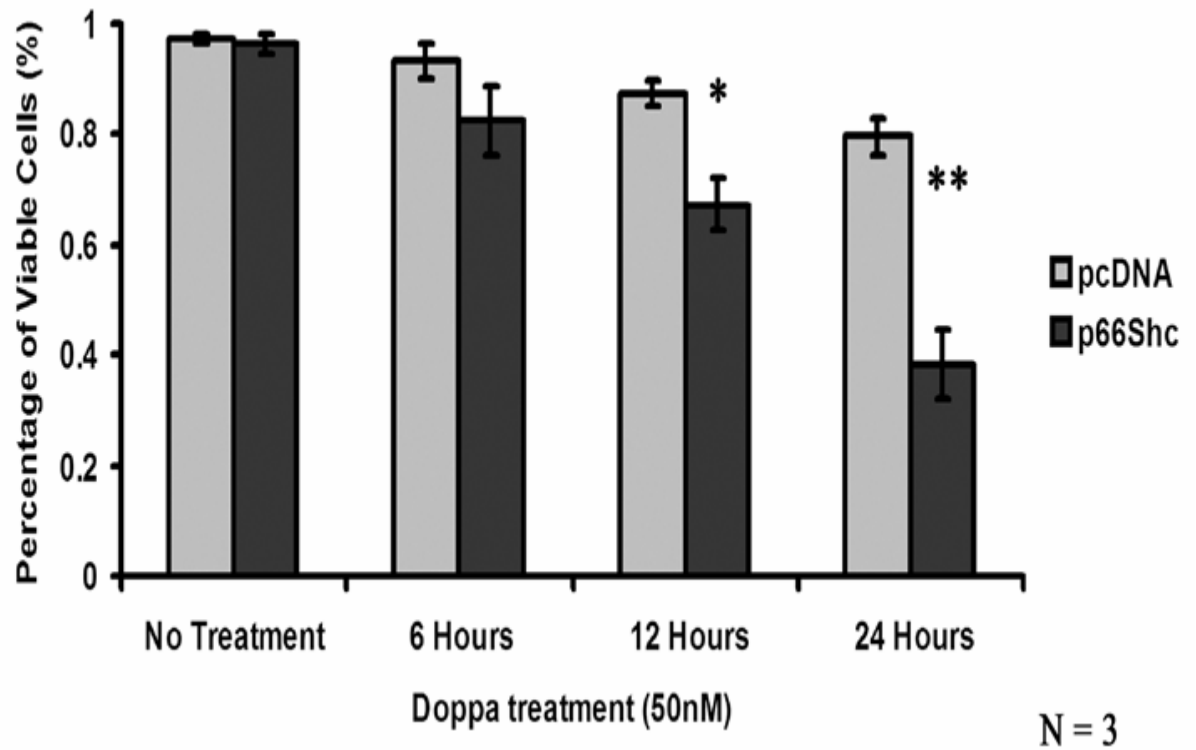


Figure 5. The effect of p66Shc-HA activation on cell viability in HT-22 cells. HT-22 cells transfected with pcDNA or p66Shc-HA plasmids were exposed to DOPPA treatment (50nM) for various times and cell viability was assessed by trypan blue dye exclusion. At 12 and 24 hours a significant decrease in cell viability was observed in DOPPA treated p66Shc-HA transfected cells compared to the pcDNA control (*, $P<0.05$; **, $P<0.01$).

Figure 5



3.5 p66Shc mediated changes in the mitochondrial disulfide proteome

Once the optimal DOPPA concentration and exposure time for activation of p66Shc were determined, it was of interest to determine the effect of p66Shc activation on the disulfide proteome in both mitochondrial and cytosolic fractions. HT-22 cells were transfected with either pcDNA3.1 or p66Shc-HA vectors, and following 50 nM DOPPA treatment for 12 hours, cellular fractionation was performed using a commercial kit. The purity of mitochondrial fractions was verified by Western blotting using an anti-VDAC antibody, which recognizes the exclusively mitochondrial localized protein (Figure 6B). Once the purity of the mitochondrial samples were established, they were resolved by Redox 2D PAGE, followed by silver staining to reveal DSBPs that were altered in a p66Shc dependent manner. In silver stained gels, a prominent diagonal band appears in both the pcDNA (control) and p66Shc-HA resolved samples, and represents proteins that did not undergo disulfide bonding (Figure 6A). Of particular interest in this experiment, are the changes that occur to the off-diagonal spots, with spots to the right of the diagonal representing inter-molecular DSBPs and spots to the left of the diagonal representing intra-molecular DSBPs. Mitochondrial samples showed relatively few protein shifts representing change in DSBP status, however, three DSBPs appeared to be altered in p66Shc-HA samples compared to the pcDNA control samples (Figure 6A). Gels were repeated in triplicate to ensure consistency of results.

3.6 Identifying mitochondrial-associated DSBPs altered with p66Shc expression

The spots in the silver stained gels that exhibited shifted or changed staining intensity in p66Shc-HA samples were excised, digested with trypsin and identified by

matrix-assisted laser desorption/ionization time-of-flight (MALDI-TOF) mass spectrometry. The three mitochondrial inter-molecular DSBPs were identified as Lamin B1 (LMNB1), peroxiredoxin1 (PRXI) and eukaryotic translation elongation factor 1 alpha (eEF1 α 1) (Table 1).

3.7 Identification of Cytosolic DSBPs Altered with p66Shc Activation

Changes in the disulfide proteome of the cytosolic fractions of HT-22 cells were also analyzed by Redox 2D-PAGE. As seen previously with Redox 2D PAGE analysis of mitochondrial fractions, a prominent diagonal band was also observed in the silver-stained 2D gels with off-diagonal spots representing DSBPs. In contrast to mitochondria extracts, many more cytosolic inter- and intra-molecular DSBPs were detected by Redox 2D-PAGE (Figure 7). However, only 5 DSBPs were reproducibly altered in p66Shc expressing HT-22 cells. MALDI-TOF MS analysis identified these proteins as tropomyosin-3 (TPM-3), aldo-keto reductase, moesin, radixin and adenylated cyclase associated protein 1 (CAP 1) (Table 2).

Figure 6. Ectopic p66Shc overexpression alters the mitochondrial disulfide proteome in HT-22 cells. HT-22 cells transfected with pcDNA and p66Shc-HA plasmids were treated with 50 nM DOPPA for 12 hours followed by subcellular fractionation to isolate mitochondria. Isolated mitochondria from both transfections were resolved by Redox 2D PAGE and silver stained to visualize proteins. A prominent diagonal band seen in both gels represent non-disulfide linked proteins, along with dark spots that appear off the diagonal regions which contain disulfide bonded proteins. Proteins that reproducibly appeared to undergo disulfide linkage following p66Shc overexpression and DOPPA treatment (50 nM) (spots 1-3, lamin B1, peroxiredoxinI and eukaryotic translation elongation factor 1 alpha 1, respectively) when compared to pcDNA transfected and DOPPA treated (50 nM) cells were identified by MALDI-TOF MS (Table 1). In the lower panel the purity of mitochondrial and cytosolic samples were verified by Western blot analysis using an antibody that recognizes the mitochondrial localized protein VDAC. VDAC protein was detected in mitochondrial, but not cytosolic fractions. Gel is representative of 3 separate experiments (N=3).

Figure 6

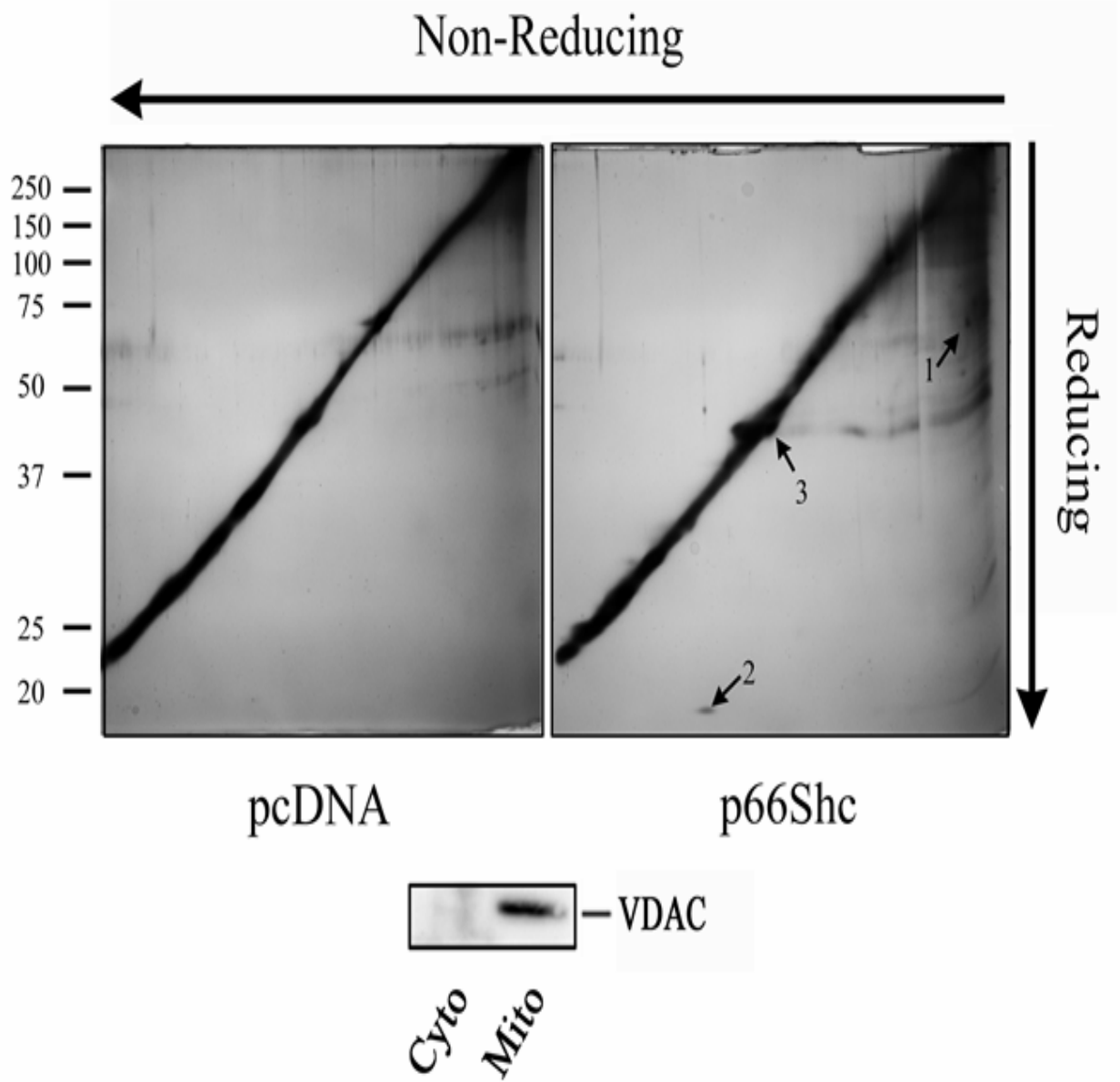


Table 1. Identification of mitochondrial disulfide linked proteins altered by p66Shc overexpression and DOPPA treatment (50 nM) in HT-22 cells.

Spot No.	Protein	Presumed Location	MOWSE Score	Function	Relative Change
1	Lamin B1	Nuclear Mitochondria	98	Nuclear Matrix Protein	Increase
2	Peroxisredoxin 1	Cytosol Mitochondria	80	Antioxidant Enzymes	Increase
3	Eukaryotic translation elongation factor 1 alpha 1	Cytosol	53	tRNA transfer/ Exports Nuclear Proteins	Increase

Mitochondrial DSBPs identified as unique to p66Shc-HA expressing HT-22 cells in Figure 6 were identified by MALDI-TOF MS. Peptide masses were searched in the NCBI RefSeq database, restricted to *Mus musculus* (house mouse) sequences, and MOWSE probability was calculated and expressed as $-10\log P$.

Figure 7. Ectopic p66Shc overexpression alters the disulfide proteome in HT-22 cytosolic fractions. HT-22 cells transfected with pcDNA and p66Shc-HA were treated with 50 nM DOPPA for 12 hours followed by cytosolic fractionation. Cytosolic protein extracts were resolved by redox 2D PAGE and silver stained to visualize proteins. A prominent diagonal band seen in both gels represents non-disulfide linked proteins, whereas dark spots that appear in off-diagonal regions contain intra- and inter-molecular disulfide bonded proteins. Proteins that reproducibly appeared to undergo disulfide linkage with p66Shc overexpression and DOPPA treatment (50 nM) (spots 1-5, tropomyosin-3, aldo-keto reductase, adenylated cyclase associated protein 1, moesin and radixin, respectively) when compared to DOPPA treated (50 nM) control (pcDNA) samples, were identified by MALDI-TOF MS (Table 2). In the lower panel the purity of cytosolic samples were verified by Western blot analysis using an antibody that recognizes the cytosolic protein actin. Gel is representative of 3 separate experiments (N=3).

Figure 7

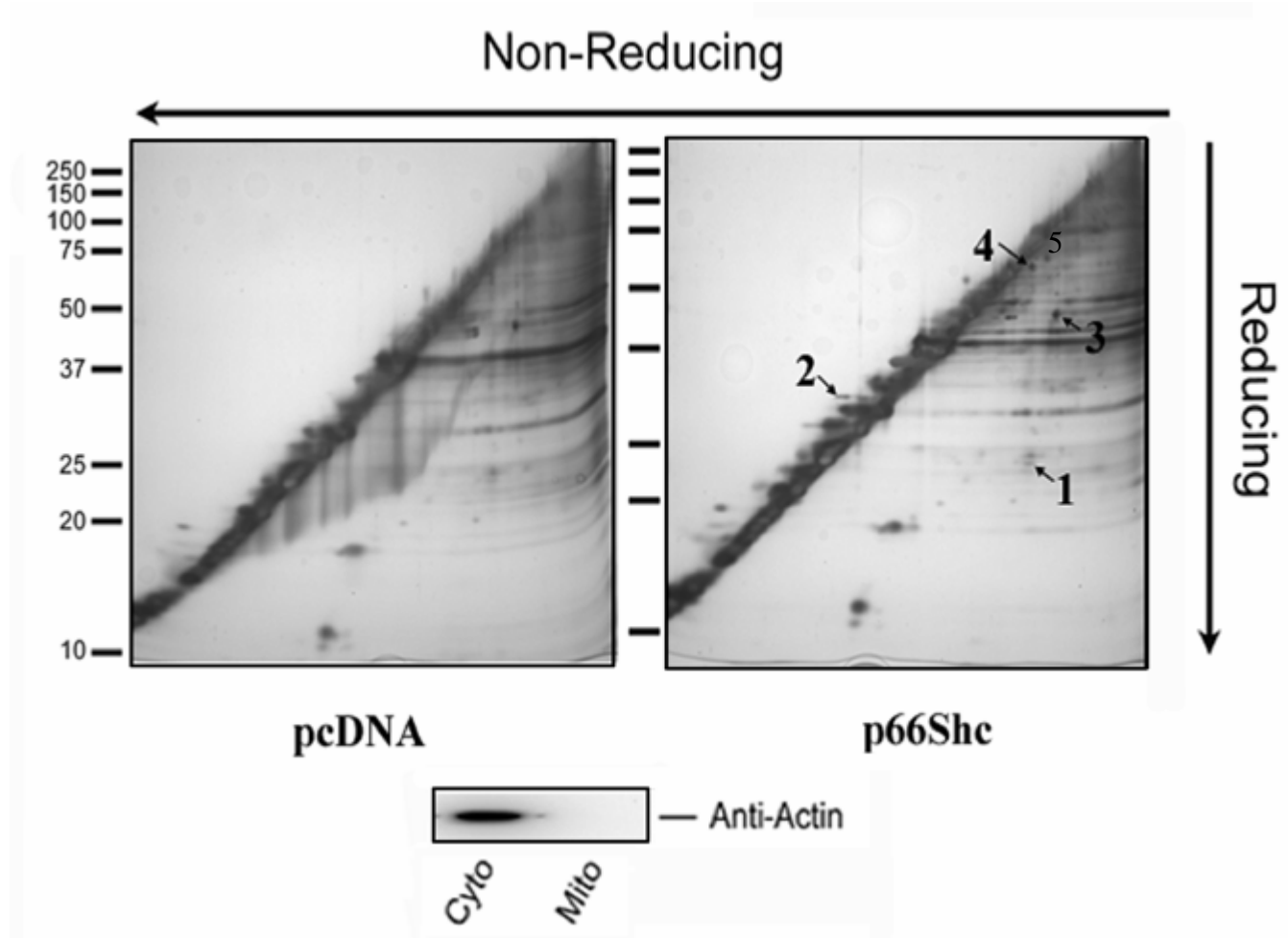


Table 2. Identification of cytosolic disulfide linked proteins altered by p66Shc overexpression and DOPPA treatment (50 nM) in HT-22 cells.

Spot No.	Protein	Location	MOWSE Score	Function	Relative Change
1	Tropomyosin 3	Cytosolic	130	Actin Binding/Cell Motility	Increase
2	Aldo-keto Reductase	Cytosolic	98	NADPH-dependent oxidoreductases	Increase
3	CAP-adenylated cyclase-associated protein	Cytosolic	82	Actin Remodeling/Cell Morphology	Increase
4	Moesin	Cytosolic	76	Actin Binding/Cell Motility	Increase
5	Radixin	Cytosolic	52	Actin Binding/Cell Motility	Increase

Alterations in disulfide linked proteins within HT-22 cytosolic samples as a result of p66Shc overexpression (Figure 7) were determined by MALDI-TOF MS. Protein sequences were BLAST searched and Peptide masses were searched in the NCBI RefSeq database, restricted to *Mus musculus* (house mouse) sequences, and MOWSE probability was calculated and expressed as $-10\log p$.

3.8 p66Shc overexpression affects the redox status of Tropomyosin-3 in the cytosol

Redox 2D PAGE analysis of HT-22 cytosolic samples identified a number of actin binding proteins, including tropomyosin-3 (TPM-3), that were affected by p66Shc expression and phosphorylation. Therefore, a non-reducing/reducing 1D SDS PAGE was performed to detect a shift in TPM-3 molecular weight indicating a change in oxidation status. Proteins that form intermolecular disulfide bonds exhibit slower electrophoretic migration and therefore appear as higher molecular weight (HMW) bands compared to the fully reduced monomeric form of the protein (Cumming et al., 2004). HT-22 cytosolic samples were resolved by both non-reducing and reducing 1D-PAGE and electroblotted onto PVDF. Blots were then probed with an anti-TPM-3 antibody to detect changes in TPM-3 disulfide bonding. P66Shc-HA expression promoted increased disulfide linked HMW forms of TPM-3 of approximately 80-90 kDa that were not apparent in the pcDNA control transfected cells (Figure 8). In addition, activation of p66Shc by DOPPA treatment further promoted increased TPM-3 disulfide linkage. In contrast, reducing 1D SDS PAGE analysis revealed that overall monomeric (~33 kDa) TPM-3 levels remain relatively constant across all treatments (Figure 8).

3.9 Changes in Filamentous Actin organization following p66Shc overexpression

TPM-3 is a non-muscle tropomyosin isoform that forms coiled-coil dimers that bind along the length of actin filaments thereby affecting cytoskeletal dynamics and cell migration (Lin, Eppinga, Warren, & McCrae, 2008). Radixin and moesin (part of the ERM family of proteins) associate with the actin cytoskeleton and plasma membrane adhesion complexes and control a variety of cellular processes including cell

morphogenesis, migration, proliferation and survival (Fehon, McClatchey, & Bretscher, 2010). CAP1 is a bifunctional protein with an N-terminal domain that binds to Ras-responsive adenyl cyclase and a C-terminal domain that inhibits actin polymerization and is important for cell morphology, migration and endocytosis (Hubberstey & Mottillo, 2002). In light of the fact that all of these proteins interact with and affect actin polymerization, and exhibit changes in disulfide linkage following p66Shc activation, it was therefore of interest to examine filamentous (F-actin) structures in HT-22 cells.

To examine changes in F-actin structure associated with p66Shc-HA activation, control (pcDNA 3.1) and experimental (p66Shc-HA) transfected HT-22 cells were treated with 50 nM DOPPA (NT, 6hrs, 12hrs), fixed, and stained with TRITC conjugated phalloidin. Phalloidin is a molecule that binds F-actin and conjugated TRITC allows for visualization by fluorescence microscopy. Staining revealed qualitative differences in F-actin structure between control and p66Shc-HA transfected cells (Figure 9). Notable changes in HT-22 cells expressing activated p66Shc-HA included a decrease in cortical actin filaments and the accumulation of peri-nuclear actin aggregates (Figure 9). It is unclear if ectopically expressed p66Shc-HA promotes alterations in F-actin through direct interaction or if changes are occurring as a result of p66Shc mediated mitochondrial ROS production. However, these results suggest that p66Shc expression and phosphorylation either directly or indirectly lead to detrimental alterations in HT-22 F-actin dynamics.

Figure 8. Overexpression of p66Shc-HA promotes increased disulfide linkage of cytosolic Tpm-3. Cytosolic extracts from pcDNA and p66Shc-HA transfected cells were resolved by non-reducing and reducing 1D SDS PAGE followed by immunoblot analysis using an anti-TPM3 antibody. HT-22 cells overexpressing p66Shc exhibited disulfide linked HMW forms of TPM-3 (~80 and 90 kDa) that were further increased following DOPPA treatment (arrows). Control cells transfected with pcDNA3.1 did not display the HMW disulfide-linked TPM-3 species in either the presence or absence of DOPPA exposure. HT-22 cytosolic fractions exposed to reducing agents displayed relatively equal levels of monomeric (33 kDa) TPM-3 in both pcDNA and p66Shc-HA transfected cells (arrowhead).

Figure 8

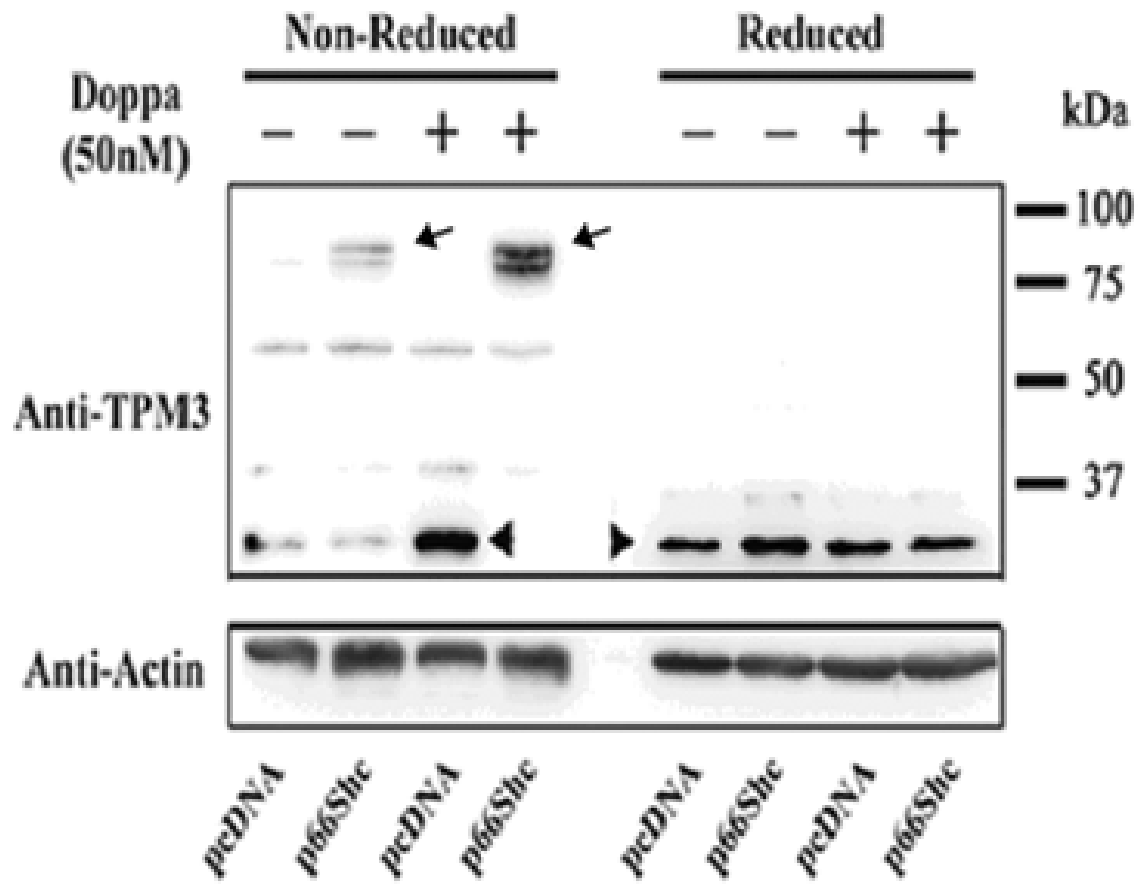
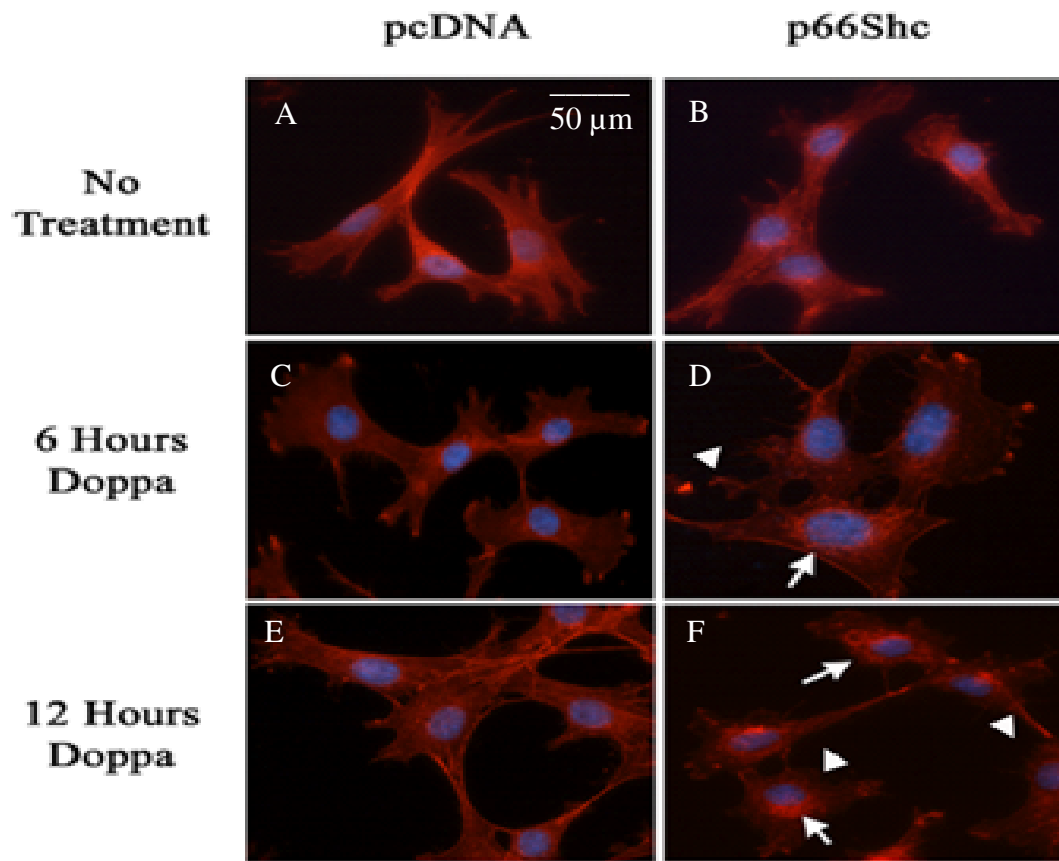


Figure 9. p66Shc activation in HT-22 cells promotes alterations in F-actin consistent with altered disulfide bonding of cytoskeletal regulators. HT-22 cells transfected with p66Shc-HA combined with DOPPA (50 nM) treatment exhibited peri-nuclear F-actin aggregates (arrows), that were absent in control transfected cells treated with DOPPA (C, E). In addition, p66Shc-HA transfected (B, D, and F) displayed a decrease in cortical actin filaments and leading edge lamellipodia structures that became more pronounced with DOPPA exposure. Arrows indicate peri-nuclear accumulations of F-actin in panels D and F, while arrowheads indicate change in cortical actin filaments and leading edge lamellipodia structures (D and F) associated with p66Shc-HA transfection and DOPPA exposure.

Figure 9



Chapter 4

Discussion and Future Research

4.1 Overview

The observation that p66Shc^{-/-} mice show significantly decreased intracellular ROS levels and increased longevity is an intriguing finding, but the molecular mechanisms underpinning this novel phenotype is poorly understood (Migliaccio et al., 1999) In this study, I sought to determine the effects of p66Shc expression on the disulfide proteome in both the mitochondria and cytoplasm of HT-22 cells. These two subcellular regions were investigated separately in hopes of identifying changes in the disulfide proteome that may be associated with redox-regulated pathways or apoptotic responses affected by p66Shc activation. The findings presented here suggest that mitochondrial DSBPs altered by p66Shc activation appear to be proteins that are traditionally found elsewhere in the cell and may localize to mitochondria through some kind of stress response mechanism. Furthermore, proteins identified to undergo altered disulfide bonding in the cytoplasm in a p66Shc-dependent manner are associated with F-actin and participate in cytoskeleton remodeling.

4.2 Overexpressing p66Shc increases ROS and decreases cell viability

The observed increase in mitochondrial ROS production occurred in p66Shc-HA transfected HT-22 cells treated with PKC- β agonist DOPPA (50 nM) for 12 hours. The increase in mitochondrial ROS production appears to be directly related to the expression and phosphorylation of p66Shc. These results are in accordance with previous p66Shc overexpression experiments performed in various mouse fibroblast and hepatocyte cells

whereby p66Shc serine phosphorylation was induced by H₂O₂ treatment (Giorgio et al., 2005; Nemoto et al., 2006). As previously discussed, p66Shc participates in redox processes and once translocated into the mitochondrial IMS, can accept electrons from cytochrome c (Gertz et al., 2008; Giorgio et al., 2005). However elevated p66Shc levels in the mitochondrial IMS are believed to decrease the efficiency of electron transport within the ETC and promote the formation of O₂⁻ and H₂O₂ (Giorgio et al., 2005; Pinton & Rizzuto, 2008). The increase in p66Shc mediated mitochondrial ROS is believed to be critical for induction of apoptosis (Migliaccio et al., 1999). These findings suggest that elevated ROS precedes cell death in the HT-22 cell model and the time-delay may be due to redox-dependent signaling processes that need to occur before initiation of cell death.

4.3 p66Shc mediated alterations in the mitochondrial disulfide proteome

Recent studies have indicated that oxidation of protein thiol groups within the mitochondrial IMS may affect cellular functions such as apoptosis and ROS homeostasis (Herrmann & Riemer, 2010). Based on previous research highlighting the ROS promoting effects of p66Shc in the mitochondrial IMS, I analyzed the disulfide proteome in isolated mitochondria from p66Shc-HA transfected HT-22 cells. This was not an easy endeavour since isolating mitochondria *in vitro* requires a large number of cells and extra caution as pelleted mitochondria are barely visible during fractionation. However, enough mitochondria were eventually isolated to resolve DSBPs via Redox 2D SDS PAGE and identify three proteins (Lamin B1 (LMNB1), Peroxiredoxin I (PRXI), Eukaryotic translation elongation factor 1 alpha 1 (eEF1 α 1)) that were altered with p66Shc activation. Interestingly, the localization of LMNB1 and PRXI to the mitochondria is of

particular interest because under normal conditions these proteins are usually found in the nucleus and cytosol, respectively.

4.3.1 Lamin B1

The identification of LMNB1 as a disulfide altered protein found localized to the mitochondria may provide a significant clue to the stress response initiated by p66Shc activation. LMNB1 is a nuclear matrix protein that is normally associated with maintaining nuclear structure and chromatin stability (Tu et al., 2012). However, recent studies suggest that under stress conditions, LMNB1 may localize to the mitochondria and play a role in apoptotic pathways (Tu et al., 2012). In a study testing the liposomal sodium morrhuate treatment of infantile hemangioma endothelial cells, LMNB1 was shown to localize to the mitochondria and be implicated in the activation of apoptotic and necrotic pathways in exposed infantile hemangioma endothelial cells (Tu et al., 2012). Interestingly, a recent study revealed that Lamin B2 (LMNB2) in cultured *Xenopus* retinal ganglion cell neurons is synthesized in close proximity to mitochondria in axons in response to guidance cue stimulation (Yoon et al., 2012). In addition, loss of axonal LMNB2 leads to mitochondria dysfunction and axon degeneration independently from the cell body. Furthermore, LMNB1 was suggested to play a role in necrosis and apoptosis in mouse cancer cell lines. An upregulation of the nuclear matrix protein was observed during 5-fluoro-2-deoxyuridine induced necrosis and apoptosis, prompting the authors of this study to speculate that LMNB1 may play a role in regulating cell death (Sato et al., 2009). The specific role of LMNB1 in regulating nerve cell function, cell morphology and apoptosis is not certain; however the research shown here suggests a change in the disulfide-linked state of LMNB1, mediated by a p66Shc-associated ROS

increase, may be responsible for initiating the localization of LMNB1 to the mitochondria.

4.3.2 Peroxiredoxin I

The identification of PRXI as a disulfide-linked protein in p66Shc overexpressing HT-22 mitochondrial fractions was of interest. Peroxiredoxins (PRXs) function as anti-oxidant enzymes that detoxify peroxides and are regulated by changes in phosphorylation, redox status and oligomerization states (Wood *et al.* 2003). PRXs are ubiquitously expressed with various isoforms localized to different subcellular compartments. In mammalian cells, there are 6 different PRX isoforms. PRXI is generally found in the cytoplasm while PRXIII is localized to the mitochondria (Fujii & Ikeda, 2002). Interestingly, a disulfide-linked form of PRXI was found in isolated mitochondria from HT-22 cells expressing activated p66Shc (Figure 6, spot 1). One possible explanation for this occurrence may relate to the activity of sulfiredoxin (SRX), an enzyme that catalyzes the reduction of cysteine sulfonic acids to an active thiol form. SRX has been shown to interact with and reduce PRXI in the cytosol, and can also translocate into the mitochondria to reduce hyper-oxidized PRXIII as an anti-apoptotic defense (Noh, Baek, Jeong, Rhee, & Chang, 2009). Therefore, the interaction of PRXI and SRX along with the localization of SRX to mitochondria under a stress response could potentially influence localization of PRXI to mitochondria; however this idea awaits further investigation. Interestingly, in a recent study PRXI was shown to interact with p66Shc in the cytoplasm (Gertz *et al.*, 2009). Interaction with PRXI leads to a reduction in p66Shc tetramer formation, which reduces its ability to induce mitochondrial

apoptosis (Gertz et al., 2009). It is uncertain if p66Shc interacts with and affects the activity of PRXI in the mitochondrial IMS, but this line of investigation is worth pursuing in future studies.

4.3.3 Eukaryotic Elongation Factor 1 Alpha 1

eEF1 α 1 was originally selected as control spot, as its location on the prominent diagonal band in redox 2D PAGE gels suggests it may not undergo alterations in DSB status. eEF1 α 1 is a subunit in the elongation factor-1 complex, which delivers aminoacyl tRNAs to the ribosome (Khacho et al., 2008). Although it was identified through MS, a change in DSB status of eEF1 α 1 could not be unequivocally confirmed due to its close proximity to the diagonal line of the gel (Figure 6).

4.4 p66Shc Mediated Alterations on the Cytosolic Disulfide Proteome

In this study, four cytosolic DSBPs were shown to be influenced by p66Shc activation and are known to associate with F-actin (Amieva & Furthmayr, 1995). Moesin, radixin, adenylated cyclase-associated protein 1 (CAP1) and tropomyosin-3 (TPM-3) are well known to interact with the actin cytoskeleton and influence cell morphology and motility (Bryce et al., 2003). The altered DSB status of these proteins likely arise as a downstream result of p66Shc activation and the associated ROS production. Proteins associated with the actin cytoskeleton can have a great impact on the form and function of cytoskeleton dynamics (Bryce et al., 2003).

4.4.1 Moesin and Radixin

Moesin and radixin are generally associated with filipodia, located at the leading edge of cell motility and is part of the ERM protein family (along with ezrin)(Lankes & Furthmayr, 1991). Moesin and radixin function as a link between the actin cytoskeleton and plasma membrane, and have been implicated in cell spatial recognition and cell signaling (Lankes & Furthmayr, 1991). Moesin and radixin are suggested to have a key role in the formation of tiny projections outward from filipodia, and detect cell signals through chemotaxis. The association of moesin and radixin with F-actin is suggested to be important for relaying signals concerning the extracellular matrix and other cells (Lankes & Furthmayr, 1991). The results presented here are the first to suggest that both proteins undergo disulfide bonding in response to elevated ROS.

4.4.2 Cyclase Associated Protein 1 (CAP1)

Cyclase associated protein 1 (CAP1) has been implicated in signaling related to filamentous actin polymerization in mammals (Hubberstey & Mottillo, 2002). CAPs possess a conserved C-terminus motif that allow interaction with filamentous actin, while the N-terminus is specified for signal relay (Hubberstey & Mottillo, 2002). Recent research has suggested that CAPs are necessary for quick depolymerisation of F-actin. CAP1 may also augment cofilin function and effectively increase the speed of F-actin depolymerisation (Normoyle & Briher, 2012). An alteration to the disulfide status of moesin, radixin and CAP1 could have large implications in dynamic cytoskeleton remodelling, cell movement and cell signaling.

4.4.3 Tropomyosin-3

Tropomyosin-3 (TPM-3) was a cytoskeleton DSBP that had the highest MOWSE sequence probability match of all the proteins identified (Table 2). TPM-3 plays an important role in actin dynamics as its primary role is to bind F-actin and inhibit access to catalytic sites in the major groove (Bryce et al., 2003). Although the specific interactions of TPM-3 in non-muscle cell actin stabilization are not as well understood as in muscle cells, studies suggest that TPM-3 provides a balance against competitor proteins such as cofilin and Arp 2/3 to help stabilize actin dynamics (DesMarais *et al.* 2005). A change in the DSB status of TPM-3 may alter protein function so that TPM-3 becomes more tightly bound to F-actin thereby causing it to become rigid and vulnerable to disorganization (Chountala, Vakaloglou, & Zervas, 2012). The functionality of TPM-3 relies heavily on its ability to dimerize through the formation of a disulfide bridge between centrally located cysteine residues, which may be controlled through a change in redox status (Hegmann, Lin, & Lin, 1988).

4.5 Non-reducing/Reducing Behaviour of Tpm-3 in p66Shc Expression Samples

The accumulation of oxidized TPM-3 in p66Shc expressing HT-22 cells suggests that stabilization of its dimerized form, effectively renders F-actin in a more rigid state (Mello et al., 2007). As previously mentioned, the dynamic nature of filamentous actin is crucial to several intracellular functions, including cell structure and motility, cell signaling, intracellular transport, endocytosis and compartmentalization of subcellular organelles (Halpain, 2003). Inhibition of actin dynamics can potentially lead to a disorganization of filamentous actin triggering stress responses and apoptosis as seen in *Drosophila* when

overexpressing the actin-binding protein parvin (Chountala et al., 2012). The changes in DSB status of actin binding proteins may help to mediate apoptotic events associated with p66Shc expression and serine phosphorylation. Increases in mitochondrial ROS formation appear to act downstream of the mitochondria, affecting actin dynamics through redox signaling, and effectively disrupting several important cell functions.

4.6 Cytoskeleton Structure changes with Cytosolic DSBP Alterations

With the identification of five actin binding proteins undergoing disulfide alterations in the cytosol of cells expressing activated p66Shc, I turned my attention to how the changes in DSB status of these proteins affects F-actin structure. Before staining for F-actin, I noticed changes in cell morphology in other p66Shc transfection + DOPPA experiments such as mitoTracker® ROS and trypan blue exclusion experiments. The natural, stellate morphology of HT-22 cells was replaced by a more rounded cell morphology. Staining control and p66Shc-HA transfected HT-22 cells +/- DOPPA (50 nM) with phalloidin-TRITC to visualize F-actin, revealed several abnormalities in F-actin related to p66Shc activation. Phalloidin staining revealed disorganization of actin filaments, peri-nuclear actin accumulation, a decrease in cortical actin filaments and disruption of lamellipodia (Figure 9B, 9D, 9F). These effects are unlikely to arise from DOPPA treatment as control cells transfected with pcDNA3.1 plasmid and treated with DOPPA (50 nM) displayed F-actin staining consistent with healthy motile cells (Figure 9A, C, E).

These results suggest that alterations in disulfide bonding of actin regulators may affect F-actin polymerization in a number of ways. Firstly, disorganized F-actin may occur as a result of an increased affinity of the oxidized dimeric form of TPM-3 for actin.

Previous studies have shown that overexpression of an oxidized dimeric isoform of Tm (Tm5NM1) produces a disorganized cytoskeleton in mesenchymal cells in a similar manner to the results seen with HT-22 cells (Lees et al., 2011). Altered F-actin dynamics as a result of tighter binding by TPM-3 may render the actin cytoskeleton vulnerable to disorganization events (Chountala et al., 2012). It has been suggested that elevated binding of TPM-3 to F-actin under stress conditions may be part of a cellular ATP conservation mechanism (Bernstein, Chen, Boyle, & Bamburg, 2006). ATP conservation under stress conditions is suggested to divert ATP to more essential cellular processes. Furthermore, increased disulfide linkage of CAP1 could not only have implications for F-actin related signaling, but also with F-actin polymerization dynamics. Recent studies suggest that CAPs accelerate cofilin mediated F-actin depolymerisation (Normoyle & Briher, 2012).

Alterations in both TPM-3 and CAP1 DSB status may be working in concert with one another, using redox signaling as a stress sensor to trigger a response to p66Shc mediated ROS. Downstream ROS accumulation in response to p66Shc activation could also be responsible for the observed peri-nuclear accumulation of F-actin. The observed peri-nuclear localization of F-actin may be the formation and accumulation of cofilin-actin rods that form under stress conditions (Munsie, Desmond, & Truant, 2012). Under the same ATP diversion mechanisms mentioned earlier, cofilin and actin are shuttled out of the nucleus in a rod-like state under stress conditions. Cofilin-actin rods function to prevent actin from polymerizing into new filaments and using valuable ATP (Munsie et al., 2012).

The visible change in F-actin stability at the leading edge in HT-22 cells expressing activated p66Shc may be caused, at least in part, by disulfide linkage of moesin and radixin. Moesin is generally highly localized within filopodia and function as cross-linkers between the plasma membrane and F-actin cytoskeleton (Lankes & Furthmayr, 1991). Alterations in the DSB status of moesin and radixin could inhibit its function and compromise structures associated with the leading edge of the cell associated with actin dynamics, microprojections, cell movement and morphology (Amieva & Furthmayr, 1995). Future studies will focus on the effect of disulfide-linkage of these actin binding proteins on cell morphology and migration in response to p66Shc activation.

4.7 Conclusions

The research presented provides new insight into the effects of p66Shc mediated ROS on the disulfide proteome within the mitochondria and cytosolic. Previous research demonstrated that p66Shc promotes increased intracellular ROS levels and apoptosis in response to serine-36 phosphorylation. However, potential redox mechanism(s) associated with p66Shc mitochondrial ROS accumulation and the downstream effects on protein redox status are poorly understood. Using an HT-22 mouse hippocampal neuronal-like cell line as an experimental model, p66Shc-HA was ectopically expressed and phosphorylation induced by the PKC- β agonist DOPPA. Alterations in the disulfide proteome of mitochondrial and cytosolic fractions were investigated to determine the effects of p66Shc mediated ROS on redox regulated processes in search of clues pertaining to the role of p66Shc in longevity. Increased levels of mitochondrial ROS

mediated by p66Shc activation affect the DSB status of LMNB1 and PRXI in HT-22 mitochondrial subcellular fractions. Localization of these two proteins to the mitochondria was surprising as these proteins are normally associated with the nuclear matrix and cytosol respectively. However, previous research suggests that LMNB1 may localize to the mitochondria as part of a stress response to promote activation of apoptotic pathways. I speculate that PRXI mitochondrial localization may be due to the translocation of SRX from the cytosol to the mitochondrial IMS under mitochondrial stress conditions. As previously mentioned SRX is an oxireductase that functions to maintain PRX in an active reduced state, with the ability to interact with both PRXI in the cytosol and translocate to associate with mitochondrial PRXIII. In addition, PRXI have been shown to interact with and inhibit p66Shc activation in the cytosol. Changes in DSB status of LMNB1 and PRXI could facilitate their localization to the mitochondria by a p66Shc dependent process.

Moesin, radixin, TPM-3, and CAP1 were all identified as cytosolic proteins that underwent altered disulfide bonding in response to p66Shc activation. In light of the role these proteins play in F-actin dynamics, these results are significant in the search for clues regarding p66Shc's role in longevity. Changes in redox status of these cytoskeletal proteins may signal a cascade of changes to F-actin dynamics and conservation of ATP in an attempt to counter p66Shc mediated perturbations of mitochondrial activity and ROS production. My research suggests that p66Shc may elicit a stress response by promoting altered disulfide bonding of proteins implicated in cytoskeletal remodeling and by facilitating the localization of disulfide-linked apoptotic proteins to the mitochondria.

References

- Amieva, M. R., & Furthmayr, H. (1995). Subcellular localization of moesin in dynamic filopodia, retraction fibers, and other structures involved in substrate exploration, attachment, and cell-cell contacts. *Exp Cell Res*, *219*(1), 180-196.
- Anfinsen, C. B., & Haber, E. (1961). Studies on the reduction and re-formation of protein disulfide bonds. *J Biol Chem*, *236*, 1361-1363.
- Beckman, K. B., & Ames, B. N. (1998). The free radical theory of aging matures. *Physiol Rev*, *78*(2), 547-581.
- Bernstein, B. W., Chen, H., Boyle, J. A., & Bamberg, J. R. (2006). Formation of actin-ADF/cofilin rods transiently retards decline of mitochondrial potential and ATP in stressed neurons. *Am J Physiol Cell Physiol*, *291*(5), C828-839.
- Bryce, N. S., Schevzov, G., Ferguson, V., Percival, J. M., Lin, J. J., Matsumura, F., . . . Weinberger, R. P. (2003). Specification of actin filament function and molecular composition by tropomyosin isoforms. *Mol Biol Cell*, *14*(3), 1002-1016.
- Carpi, A., Menabo, R., Kaludercic, N., Pelicci, P., Di Lisa, F., & Giorgio, M. (2009). The cardioprotective effects elicited by p66(Shc) ablation demonstrate the crucial role of mitochondrial ROS formation in ischemia/reperfusion injury. *Biochim Biophys Acta*, *1787*(7), 774-780.
- Chountala, Maria, Vakaloglou, Katerina M., & Zervas, Christos G. (2012). Parvin Overexpression Uncovers Tissue-Specific Genetic Pathways and Disrupts F-Actin to Induce Apoptosis in the Developing Epithelia in Drosophila. *PLoS ONE*, *7*(10), e47355.
- Cumming, R. C., Andon, N. L., Haynes, P. A., Park, M., Fischer, W. H., & Schubert, D. (2004). Protein disulfide bond formation in the cytoplasm during oxidative stress. *J Biol Chem*, *279*(21), 21749-21758.
- DesMarais, V., Ghosh, M., Eddy, R., & Condeelis, J. (2005). Cofilin takes the lead. *J Cell Sci*, *118*(Pt 1), 19-26.
- Di Lisa, F., Kaludercic, N., Carpi, A., Menabo, R., & Giorgio, M. (2009). Mitochondrial pathways for ROS formation and myocardial injury: the relevance of p66(Shc) and monoamine oxidase. *Basic Res Cardiol*, *104*(2), 131-139.

- Fehon, R. G., McClatchey, A. I., & Bretscher, A. (2010). Organizing the cell cortex: the role of ERM proteins. *Nat Rev Mol Cell Biol*, *11*(4), 276-287.
- Fujii, J., & Ikeda, Y. (2002). Advances in our understanding of peroxiredoxin, a multifunctional, mammalian redox protein. *Redox Rep*, *7*(3), 123-130.
- Fulda, S., Gorman, A. M., Hori, O., & Samali, A. (2010). Cellular stress responses: cell survival and cell death. *Int J Cell Biol*, *2010*, 214074.
- Gertz, M., Fischer, F., Leipelt, M., Wolters, D., & Steegborn, C. (2009). Identification of Peroxiredoxin 1 as a novel interaction partner for the lifespan regulator protein p66Shc. *Aging (Albany NY)*, *1*(2), 254-265.
- Gertz, M., Fischer, F., Wolters, D., & Steegborn, C. (2008). Activation of the lifespan regulator p66Shc through reversible disulfide bond formation. *Proc Natl Acad Sci U S A*, *105*(15), 5705-5709.
- Giorgio, M., Migliaccio, E., Orsini, F., Paolucci, D., Moroni, M., Contursi, C., Pelicci, P. G. (2005). Electron transfer between cytochrome c and p66Shc generates reactive oxygen species that trigger mitochondrial apoptosis. *Cell*, *122*(2), 221-233.
- Gschwendt, M., Kittstein, W., & Marks, F. (1991). Protein kinase C activation by phorbol esters: do cysteine-rich regions and pseudosubstrates play a role? *Trends Biochem Sci*, *16*(5), 167-169.
- Halpain, S. (2003). Actin in a supporting role. *Nat Neurosci*, *6*(2), 101-102. Hegmann, T. E., Lin, J. L., & Lin, J. J. (1988). Motility-dependence of the heterogenous staining of culture cells by a monoclonal anti-tropomyosin antibody. *J Cell Biol*, *106*(2), 385-393.
- Herrmann, J. M., & Riemer, J. (2010). Oxidation and reduction of cysteines in the intermembrane space of mitochondria: multiple facets of redox control. *Antioxid Redox Signal*, *13*(9), 1323-1326.
- Hubberstey, A. V., & Mottillo, E. P. (2002). Cyclase-associated proteins: CAPacity for linking signal transduction and actin polymerization. *FASEB J*, *16*(6), 487-499.
- Inaba, K. (2010). Structural basis of protein disulfide bond generation in the cell. *Genes Cells*, *15*(9), 935-943.

- Khacho, M., Mekhail, K., Pilon-Larose, K., Pause, A., Cote, J., & Lee, S. (2008). eEF1A is a novel component of the mammalian nuclear protein export machinery. *Mol Biol Cell*, *19*(12), 5296-5308.
- Lankes, W. T., & Furthmayr, H. (1991). Moesin: a member of the protein 4.1-talin-ezrin family of proteins. *Proc Natl Acad Sci U S A*, *88*(19), 8297-8301.
- Lees, J. G., Bach, C. T., Bradbury, P., Paul, A., Gunning, P. W., & O'Neill, G. M. (2011). The actin-associating protein Tm5NM1 blocks mesenchymal motility without transition to amoeboid motility. *Oncogene*, *30*(10), 1241-1251.
- Lin, J. J., Eppinga, R. D., Warren, K. S., & McCrae, K. R. (2008). Human tropomyosin isoforms in the regulation of cytoskeleton functions. *Adv Exp Med Biol*, *644*, 201-222.
- Lombard, D. B., Chua, K. F., Mostoslavsky, R., Franco, S., Gostissa, M., & Alt, F. W. (2005). DNA repair, genome stability, and aging. *Cell*, *120*(4), 497-512.
- Mello, C. F., Sultana, R., Piroddi, M., Cai, J., Pierce, W. M., Klein, J. B., & Butterfield, D. A. (2007). Acrolein induces selective protein carbonylation in synaptosomes. *Neuroscience*, *147*(3), 674-679.
- Migliaccio, E., Giorgio, M., Mele, S., Pelicci, G., Reboldi, P., Pandolfi, P. Pelicci, P. G. (1999). The p66shc adaptor protein controls oxidative stress response and life span in mammals. *Nature*, *402*(6759), 309-313.
- Munsie, L. N., Desmond, C. R., & Truant, R. (2012). Cofilin nuclear-cytoplasmic shuttling affects cofilin-actin rod formation during stress. *J Cell Sci*, *125*(17), 3977-3988.
- Nemoto, S., Combs, C. A., French, S., Ahn, B. H., Fergusson, M. M., Balaban, R. S., & Finkel, T. (2006). The mammalian longevity-associated gene product p66shc regulates mitochondrial metabolism. *J Biol Chem*, *281*(15), 10555-10560.
- Nemoto, S., & Finkel, T. (2002). Redox regulation of forkhead proteins through a p66shc-dependent signaling pathway. *Science*, *295*(5564), 2450-2452.
- Noh, Y. H., Baek, J. Y., Jeong, W., Rhee, S. G., & Chang, T. S. (2009). Sulfiredoxin Translocation into Mitochondria Plays a Crucial Role in Reducing Hyperoxidized Peroxiredoxin III. *J Biol Chem*, *284*(13), 8470-8477.

- Normoyle, K. P., & Briehar, W. M. (2012). Cyclase-associated Protein (CAP) Acts Directly on F-actin to Accelerate Cofilin-mediated Actin Severing across the Range of Physiological pH. *J Biol Chem*, 287(42), 35722-35732.
- Novo, E., & Parola, M. (2008). Redox mechanisms in hepatic chronic wound healing and fibrogenesis. *Fibrogenesis Tissue Repair*, 1(1), 5.
- Pani, G., Koch, O. R., & Galeotti, T. (2009). The p53-p66shc-Manganese Superoxide Dismutase (MnSOD) network: a mitochondrial intrigue to generate reactive oxygen species. *Int J Biochem Cell Biol*, 41(5), 1002-1005.
- Paulsen, C. E., & Carroll, K. S. (2010). Orchestrating redox signaling networks through regulatory cysteine switches. *ACS Chem Biol*, 5(1), 47-62.
- Pelicci, Giuliana, Lanfrancone, Luisa, Grignani, Francesco, McGlade, Jane, Cavallo, Federica, Forni, Guido, Giuseppe & Pelicci, Pier. (1992). A novel transforming protein (SHC) with an SH2 domain is implicated in mitogenic signal transduction. *Cell*, 70(1), 93-104.
- Pinton, P., & Rizzuto, R. (2008). p66Shc, oxidative stress and aging: importing a lifespan determinant into mitochondria. *Cell Cycle*, 7(3), 304-308.
- Rabilloud, T., Chevallet, M., Luche, S., & Leize-Wagner, E. (2005). Oxidative stress response: a proteomic view. *Expert Rev Proteomics*, 2(6), 949-956.
- Ray, P. D., Huang, B. W., & Tsuji, Y. (2012). Reactive oxygen species (ROS) homeostasis and redox regulation in cellular signaling. *Cell Signal*, 24(5), 981-990.
- Rety, S., Futterer, K., Grucza, R. A., Munoz, C. M., Frazier, W. A., & Waksman, G. (1996). pH-Dependent self-association of the Src homology 2 (SH2) domain of the Src homologous and collagen-like (SHC) protein. *Protein Sci*, 5(3), 405-413.
- Ryves, W. J., Evans, A. T., Olivier, A. R., Parker, P. J., & Evans, F. J. (1991). Activation of the PKC-isotypes alpha, beta 1, gamma, delta and epsilon by phorbol esters of different biological activities. *FEBS Lett*, 288(1-2), 5-9.
- Samali, A., Fulda, S., Gorman, A. M., Hori, O., & Srinivasula, S. M. (2010). Cell stress and cell death. *Int J Cell Biol*, 2010, 245803.
- Sato, A., Satake, A., Hiramoto, A., Okamatsu, A., Nakama, K., Kim, H. S., & Wataya, Y. (2009). Association of nuclear-intermediate filament lamin B1 with necrotic- and

- apoptotic-morphologies in cell death induced by 5-fluoro-2'-deoxyuridine. *Nucleic Acids Symp Ser (Oxf)*(53), 293-294.
- Sena, L. A., & Chandel, N. S. (2012). Physiological roles of mitochondrial reactive oxygen species. *Mol Cell*, 48(2), 158-167.
- Sideris, D. P., & Tokatlidis, K. (2010). Oxidative protein folding in the mitochondrial intermembrane space. *Antioxid Redox Signal*, 13(8), 1189-1204.
- Sohal, R. S., & Orr, W. C. (2012). The redox stress hypothesis of aging. *Free Radic Biol Med*, 52(3), 539-555.
- Song, G., Ouyang, G., & Bao, S. (2005). The activation of Akt/PKB signaling pathway and cell survival. *J Cell Mol Med*, 9(1), 59-71.
- Su, K., Bourdette, D., & Forte, M. (2012). Genetic inactivation of mitochondria-targeted redox enzyme p66ShcA preserves neuronal viability and mitochondrial integrity in response to oxidative challenges. *Front Physio*, 3(285), 1-9.
- Trinei, M., Berniakovich, I., Beltrami, E., Migliaccio, E., Fassina, A., Pelicci, P., & Giorgio, M. (2009). P66Shc signals to age. *Aging (Albany NY)*, 1(6), 503-510.
- Tu, J. B., Dong, Q., Hu, X. Y., Jiang, F., Ma, R. Z., He, L. Y., & Yang, Z. Q. (2012). Proteomic analysis of mitochondria from infantile hemangioma endothelial cells treated with sodium morrhuate and its liposomal formulation. *J Biochem Mol Toxicol*, 26(9), 374-380.
- Wills, M. K., & Jones, N. (2012). Teaching an old dogma new tricks: twenty years of Shc adaptor signalling. *Biochem J*, 447(1), 1-16.
- Wood, Z. A., Schroder, E., Robin Harris, J., & Poole, L. B. (2003). Structure, mechanism and regulation of peroxiredoxins. *Trends Biochem Sci*, 28(1), 32-40.
- Yoon, B. C., Jung, H., Dwivedy, A., O'Hare, C. M., Zivraj, K. H., & Holt, C. E. (2012). Local translation of extranuclear lamin B promotes axon maintenance. *Cell*, 148(4), 752-764.

TYLER CANN

EDUCATION

Master of Science, Cell and Molecular Biology - candidate

Western University

London, Ontario

2010 Bachelor of Science, Honors Specialization in Cell and Developmental Biology

Western University

London, Ontario

EMPLOYMENT

2010 – 2012 **Teaching Assistant**

Western University

London, Ontario

LABORATORY EXPERIENCE

2010-2012 Graduate Research

London, Ontario

Western University

Supervisor: Dr. Robert Cumming

Investigated intracellular reducing and oxidizing proteomics in both mitochondrial and cytosolic cellular fractions

Successfully obtained results using cell culture, cell transfection, Polymerase Chain Reactions, Western blotting, plasmid construction, and fluorescent microscopy techniques

2009-2010 Undergraduate Research

London, Ontario

Western University

Supervisor: Dr. Robert Cumming

Investigated toxicity associated with mutant huntingtin protein in a Huntington's disease cell model

Successfully created silencing ribonucleic acid constructs

Obtained results using Northern blotting, Western blotting, fluorescent microscopy and protein quantification techniques

Publications and awards

Pitts A, Dailey K, Newington JT, Chien A, Arsenault R, **Cann T**, Thompson LM, Cumming R. (2012). Dithiol-based Compounds Maintain Expression of Antioxidant Protein Peroxiredoxin 1 That Counteracts Toxicity of Mutant Huntingtin. *J Biol Chem* (287) **27**: 22717-22729.

2011 and 2012 - Nominated for Graduate Student Teaching Award - *Western University*